Direct cell-cell communication through gap junctions during early skeletal muscle development and regeneration in the rat

PhD Thesis

Anikó Görbe MD

Department of Biochemistry, Faculty of Medicine

University of Szeged, Hungary

2007

Full papers directly related to the subject of the thesis:

I. Aniko Gorbe, David L Becker, Laszlo Dux, Eva Stelkovics, Laszlo Krenacs, Eniko Bagdi, Tibor Krenacs

Transient upregulation of connexin43 gap junctions and synchronized cell cycle control precede myoblast fusion in regenerating skeletal muscle *in vivo*

Histochem Cell Biol (2005) 123:573-83

II. Aniko Gorbe, David L Becker, Laszlo Dux, Laszlo Krenacs, Tibor Krenacs

In differentiating prefusion myoblasts connexin43 gap junction coupling is upregulated before myoblast alignment then reduced in post-mitotic cells.

Histochem Cell Biol (2006) 125:705-16

III. Aniko Gorbe, Tibor Krenacs, Jeremy Cook, David L Becker

Myoblast proliferation and syncytial fusion both depend on connexin43 function in transfected skeletal muscle primary cultures.

Exp Cell Res (2007) 313:1135-48

Contents

Abbreviations

ATP	adenosine triphosphate
BSA	bovine serum albumin
cAMP	cyclic adenosine monophosphate
cGMP	cyclic guanosine monophosphate
CLSM	confocal laser scanning microscopy
Cx	connexin
dn	dominant negative
EDTA	ethylenediaminetetraacetic acid
eGFP	enhanced green fluorescence protein
FGF	fibroblast growth factor
FITC/TRITC	fluoresceine/tetramethyelrhodamine isothiocyanate
GJIC	gap junctional intercellular communication
IP3	inositol- triphosphate
MEF	myocyte enhancer factor
MPC	muscle progenitor cell
MRF	myogenic regulatory factor
NO	nitrogen-monoxide
PBS	phosphate buffered saline
PKC	protein kinase C
TBS	tris buffered saline
wt	wild type

Summary

Direct cell-cell communication via gap junction channels between adjacent cells has ubiquitous role in various physiological and pathological processes of most tissues. It is well known that gap junctional intercellular communication does not occur in adult skeletal muscle; however, it may contribute to information exchange between myoblasts during skeletal muscle development. Our aim was to study the possible role of direct cell-cell communication in the cooperation of mononuclear myogenic progenitors during their coordinated differentiation and fusion into functioning myofibers. Our concept was based on the suggestion that for a synchronized and large scale cell-membrane fusion of myoblasts, many cells formed in several series of cell cycles need to be tuned to the same differentiation stage, and that gap junctions may have the potential to fit in this coordination.

Gap junction channels are made up of transmembrane connexin proteins. First we mapped connexin expression during myoblast differentiation in Wistar rats by using two experimental models of myogenesis: *in vivo* regeneration and *in vitro* cell culture. The patterns of Cx43 expression and phenotypic myoblast maturation were highly comparable both in regenerating soleus muscle and in differentiating primary myoblasts. Early expression (from day-1) of Cx43 in the proliferating single myogenic progenitors was followed by a progressive upregulation in interacting myoblasts until syncytial fusion and then by a rapid decline in multinucleate myotubes. This was in line with mRNA expression pattern of Cx43 in the regenerating muscle model. In regeneration, the significant upregulation of Cx43 gap junctions in aligned myoblasts preceding fusion was accompanied by the widespread nuclear expression of cyclin-dependent kinase inhibitors p21$^{waf1/Cip1}$ and p27^{kip1} and the complete loss of Ki67 protein. The synchronized exit of myoblasts from the cell cycle following extensive gap junction formation suggested a role for Cx43 channels in the regulation of cell cycle control.

For functional studies, primary myoblast cultures of the same species used *in vivo* were set up, which showed very similar temporal regulation of connexin43 expression to that of the animal model. Progressive expression of Cx43 gap junctions and synchronized cell cycle arrest in pre-fusion myoblasts was correlated here with the regulation of functional cell coupling using a dye transfer assay. Functional data showed that direct cell-cell communication through gap junctions was most active in the proliferating, sparse meshworks of myoblasts and the efficiency of myoblast coupling was reduced significantly in the aligned postmitotic (but still prefusion) cells. In line with the previous findings these results are

consistent with a potential role of gap junctions in synchronizing myoblast cell cycle to assist in their coordinated syncytial fusion.

In the third part of the study, we manipulated (enhanced or inhibited) connexin expression and the consequent coupling during myogenic differentiation to see how these affect myoblast proliferation (cell number) and fusion (myotube number). Wild-type and dominant-negative connexin43 variants (wtCx43, dnCx43) were introduced into rat myoblasts in primary culture through pIRES-eGFP vector constructs. Myoblasts transfected with wtCx43 showed more gap-junctional coupling than GFP-only controls, began fusion sooner as judged by the incidence of cytoplasmic coupling, and formed more myotubes. Myoblasts transfected with dnCx43 remained proliferative for longer than either GFP-only or wtCx43 myoblasts, showed less coupling, and underwent little fusion into myotubes. These results further confirmed the importance of gap-junctional coupling in myoblast differentiation and syncytial fusion.

Introduction
Skeletal muscle development and differentiation

Overview of embryonic skeletal muscle development

Skeletal myogenesis is a complex process that begins during somitogenesis in the embryo and continues through postnatal development. During embryogenesis, skeletal muscle forms in the vertebrate limb from progenitor cells originating in the somites, which are blocks of mesodermal cells situated lateral to the neural tube in the embryo. The ventral part of the somite, called sclerotome, will form the cartilage and bone of the vertebral column and ribs, whereas the dorsal part of the somite, the dermomyotome, gives rise to the overlying derm of the back and to the skeletal muscles of the body and limbs (Tajbakhsh & Buckingham 2000). Muscle progenitor cells (MPCs) delaminate from the   axial dermomyotome and migrate into the limb field to the positions where the dorsal and ventral muscle masses will form eventually. The mesenchymal cells of the limb which are thought to provide the positional cues for MPCs coming from the somite (Christ & Ordahl 1995), which are proliferating, but not yet differentiated cells, though they are referred to as determined. Finally, myoblasts stop dividing, align, and fuse to form a syntitium and subsequently differentiate into skeletal muscle. Concomitant with cellular fusion there is a dramatic rise in the expression of genes necessary for muscle development and function.

Stages of skeletal muscle development and factors involved in its regulation

Muscles are assembled by fusion of individual postmitotic myoblasts to form multinucleated syncytial myotubes. Early myogenesis is intrinsically complex requiring a well-coordinated transition from proliferation, through migratory alignment and cycle exit, to breakdown of apposed membranes (Fig 1).
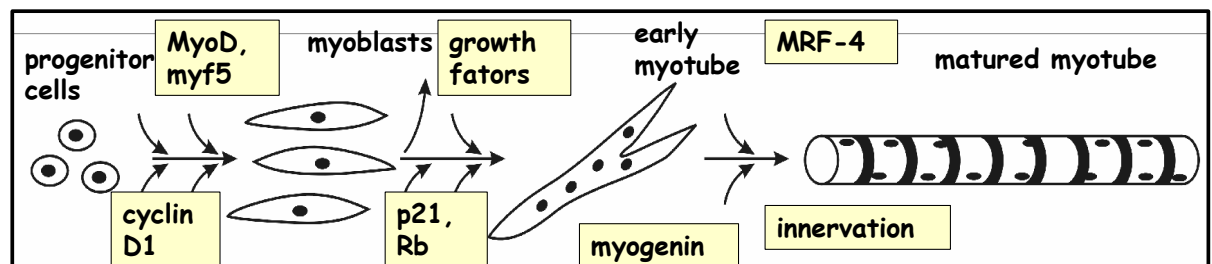

Figure 1.
Factors involved during early steps of myogenesis

The first important step of myogenesis is the formation of the MPCs/presumptive myoblasts from progenitor cells. Muscle precursors are in a stem cell like stage, with the

potential to become muscle cells. They migrate from the somite, and when reaching the limb, start to express MyoD and Myf-5 (myogenic regulatory transcription factors, [MRFs]) (Tajbakhsh and Buckingham 1994), which are responsible for myoblast determination (Rawls and Olson 1997). MRFs are basic helix–loop–helix transcription factors, acting through a conserved basic DNA binding domain that binds the E-box and form complexes with E-protein and myocyte enhancer factors (Yun and Wold 1996). MyoD and Myf5 play a critical role in myogenic commitment since no skeletal muscle forms in their double mutants because the lack of precursor myoblast population (Rudnicki et al. 1993). In their absence, cells in the somite, which would normally become myoblasts, do not locate correctly to sites of myogenesis and adopt other cell fates (Tajbakhsh et al. 1996). Migration and delamination of MPCs depend on the presence of c-met, a tyrosine kinase receptor which interacts with its ligand , called scatter factor, produced by non-somitic mesodermal cells which thus delineate the migratory route (Dietrich et al. 1999). At this stage of myogenesis, MPCs actively proliferate requiring an accurate combination of growth factors. The fibroblast growth factor (FGF) family has also been implicated in myogenesis in the limb and it has been supposed that signalling through FGF receptors promotes myoblast proliferation (Edom-Vovard et al. 2001) and even migration to the limb bud (Webb et al. 1997). These early myoblasts do not yet express a differentiated phenotype but already produce the muscle specific intermediate filament desmin (Haider et al. 1994).

Commitment to differentiation is characterised by the formation of elongated myoblasts expressing myogenin and MRF4 which are essential for terminal muscle differentiation (Rawls and Olson 1997). Activation of genes of muscle specific and cell adhesion molecules and interactions between the pathways of myogenic regulation and cell cycle control eventually result in orderly aligned myoblasts prepared for syncytial fusion (Kitzman and Fernandez 2001; Parker et al. 2003). Upregulation of $p21^{waf1/Cip1}$, a cyclin dependent kinase inhibitor, has been shown to play a key role in promoting myoblast differentiation and viability (Lawlor and Rotwein 2000; Ostrovsky and Bengal 2003). On the other hand, $p21^{waf1/Cip1}$ can be activated through gap junctional coupling in bystander cells (Azzam et al. 2001; Little et al. 2002). Furthermore, $p27^{kip1}$ another cyclin dependent kinase inhibitor can mediate the growth controlling effect of forced connexin (Cx) expression (Koffer et al. 2000). Muscle differentiation is also regulated by TGFβ and insulin-like growth factor. Optimal Ca^{++} concentration is also required at this developmental phase. Activation of Ca^{++}-dependent phosphatase, calcineurin was documented too in skeletal muscle differentiation (Friday et al. 2000) suggesting the existence of Ca^{++}-mediated signalling pathway during myoblast

differentiation. Extracellular ATP (purinergic) receptors (P2) are expressed early during embryonic muscle development. In the prefusion stage, when differentiating myoblasts become aligned and to prepare for fusion, several signalling mechanism seems to be activated. Ca^{++} activates NO synthase producing NO, which increases cGMP level (Choi et al. 1992). cAMP level increases through activation of prostaglandin receptors (David et al. 1981) and both can be an important messengers in fusion signalling.

The large-scale fusion process takes place within a narrow time frame (Rash and Fambrough 1973) and involves specific cell surface interactions between adjacent cells mediated by cadherins (Kaufmann et al. 1999) and calpains (Brustis et al. 1994) regulated by Ca^{++} dependent phosphorylation. Net calcium influx into the myoblasts is necessary for syntitia formation (David et al. 1981). The increase in intracellular Ca^{++} level is probably one of many confluent processes such as membrane hyperpolarisation and increase in cAMP through activation of prostaglandin receptors and cGMP levels that contribute to the initiation of fusion. Newly created primary myotubes act as templates for the formation of secondary myotubes lining up parallel to the primary myotube, which are multinucleated, synthesizing myofibrillar proteins to assemble into contractible myofibrils. As the myofiber matures, its contraction can be initiated by single motor neuron activity. By this time, mature myofibers express characteristic molecules for fine contractile functions, principally different myosin heavy chain isoforms and metabolic enzymes (Charge and Rudnicki 2004).

Regeneration of skeletal muscle

Mammalian skeletal muscle has the ability to complete a rapid and extensive regeneration in response to severe damage. Muscle regeneration recapitulates ontogenic muscle differentiation within a short time, offering a superb model for studying myogenesis (Lefaucheur and Sebille 1995). Different type of animal models were developed to examine muscle regeneration process, but the use of myotoxins such as bupivacaine (Marcaine), cardiotoxin, and notexin is perhaps the easiest and most reproducible way to induce muscle regeneration/differentiation (Charge and Rudnicki 2004). The snake venom notexin causes a complete and severe myonecrosis leaving the basal lamina, nerves and vessels mainly unaffected allowing for a fast and selective regeneration process of the muscles within a pre-existing scaffolding.

Resident within adult skeletal muscle, there is a pool of undifferentiated mononuclear cells termed satellite cells. They are located at the periphery of the mature multinucleated myofibers, between their sarcolemma and basal lamina (Hawke and Garry 2001) forming the

cellular basis for muscle growth and regeneration (Tajbakhsh et al. 2003). During regeneration, quescent satellite cells can be activated by damage stimuli for myogenic commitment, proliferation and differentiation to ultimately form new muscle fibers through syncytial fusion of myoblasts in regeneration (Hawke and Garry 2001). Embryonic and fetal myoblasts can be distinguished from adult muscle satellite cells based on their behaviour on differentiation signal in cell culture (Cossu & Molinaro 1987), in terms of morphological criteria, drug resistance and gene expression. The myogenic regulatory factors are also present during the formation of adult muscle fibres and can also be detected in regenerating rat muscle (Mendler et al. 1998). Myf5 (Myf5- nlacZ) is transcribed in most satellite cells (Beauchamp et al. 2000) which accumulate MyoD as differentiate. It is Pax7, which has been shown to play a crucial role in the formation of adult skeletal muscle (Seale et al. 2000).

Direct cell-cell communication through gap junctions

In regeneration and in embryonic myogenesis, the rapid formation of myotubes (Rash and Fambrough 1973) depends on an adequate supply of contiguous, fusion-competent myoblasts. This implies a near-synchronous switch from independent proliferation towards aligned differentiation across the entire population, and several lines of evidence implicate gap-junctional communication as a coordinating factor in this switch.

Gap junction structure
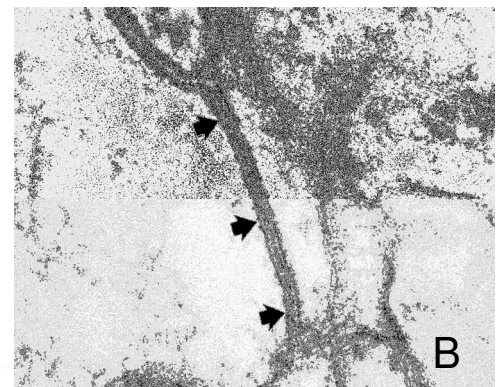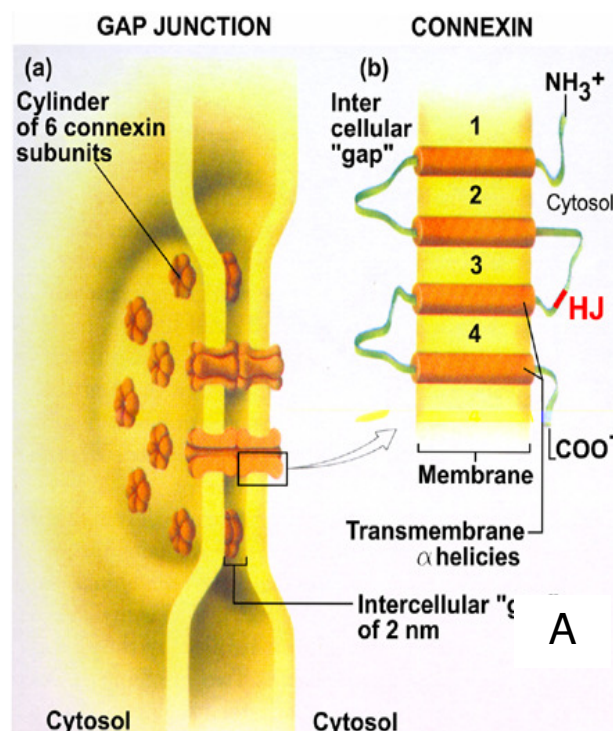
Figure 2.
(A) a) Docking of hemichannels into the plasma membrane and forming gap junction
b) Transmembrane localisation of a single connexon (Benneth et al 1991)
(B) Assembly of gap junctions in the membranes of 2 neighbouring cells (electron microscopy)

Gap junctions are intercellular channels between adjacent cells found in almost all tissues of vertebrates. Direct cell-cell communication via gap junction channels can facilitate rapid exchange of information using small molecular or ionic messengers of < 1kDa between coupled cell meshworks. The channels are formed by docking of two hemichannels (connexons) made up Cx hexamers located in the plasma membrane of adjacent cells (Paul et al. 1995, Goodenough et al. 2003) (Fig 2A). Close membrane appositions characteristic of gap junctions and their connexon plaques inserted in the plasma membranes and can be revealed using transmission and freeze fracture scanning electron microscopy (Goodenough et al. 1996) (Fig 2 B).

Connexin isotypes and their functional domains

Each connexin is named either according to its molecular weight e. g. Cx43, wich is the most conserved isotype, or based on the phylogenetic relations of connexins (Kumar et al. 1996) by grouping them into α and β classes (Fig 3A). More than 20 connexin genes have been cloned and most tissues express more than one connexin subtype (Bruzzone et al. 1996; Söhl and Willecke 2003), thus, homomeric and heteromeric connexons exist.

A

Phylogenetic relation of Cxs	Molecular mass	Examples of organs with expression
α1	Cx43	Heart
α2	Cx38	Embryo
α3	Cx46	Lens
α4	Cx37	Endothelium
α5	Cx40	Lung
α6	Cx45	Heart
α7	Cx33	Testes
α8	Cx50	Lens
α9	Cx60	Ovary
α10	Cx46.6	Cochlea
β1	Cx32	Liver
β2	Cx26	Liver
β3	Cx31	Skin
β4	Cx31.1	Skin
β5	Cx30.3	Skin
β6	Cx30	Skin, Ear

B

Figure 3.
(A) Classification of connexin isotypes (Modified from Evans and Martin 2002)
(B)Domains of connexin protein (Martin PE et al 2004)

The genomic organization of Cx genes is fairly conserved. Each Cx subtype is encoded by a separate gene located on different chromosomes with the coding region concentrated in most Cxs into a single exon. In contrast to the similarities at the level of genomic organization, the expression of Cx genes is more complex and regulated (de Maio et

al. 2002) mostly at the transcriptional level e.g. cytokines and hormones. FGF has been shown to stimulate Cx43 expression in cardiac fibroblasts (Doble and Kardami 1995). Parathyroid hormone and thyroid hormone receptors have also been reported to regulate transcription of Cx43 gene (Stock and Sies 2000).

Connexins proteins are made up of highly conserved and variable domains (Sosinsky et al. 1996). Variable regions of amino acid sequences are found in the cytoplasmic C termini, considered as the "hypervariable" segment, and the conserved regions are located in the four transmembrane domains and in the two extracellular loops (Goodenough et al. 1988, Evans et al. 1994, Duffy et al. 2002). The transmembrane domains anchor the protein into the membrane and the third intramembrane region is believed to form the inside of the channel wall (Milks et al. 1988). The extracellular domains are important in cell-to-cell recognition and docking between pairs of channels and the cytoplasmic domains influence or regulate the physiological properties of the channel (Laird et al. 1996) (Fig3B).

Assembly of functioning gap junction channels

Synthesis and formation of gap junctions take place at a rapid turnover (Fallon and Goodenough 1981). The half-life for the assembly of gap junctions in various tissues and cells has been determined as short as 1.5-3.5 hours (Laird et al. 1995). Connexins, following insertion into the endoplasmic reticulum, are delivered during assembly to the Golgi via the classical secretory pathway (Laird et al. 1996). Posttranslational modification of connexins may also occur, and phosphorylation events appear to be important in determining their structural and functional conformation, at early stages of the secretory pathway (Crow et al. 1990)

Role of gap junction communication in cell and tissue functions

Gap junction channels may provide direct pathway for small molecules (<1kD), metabolites and second messengers such as inositol-triphosphate and cAMP, and ions e.g. Ca^{++}, to rapidly pass between adjacent cells (Loewenstein et al. 1981, Kumar and Gilula 1996, Willecke et al. 2002, Evans et al. 2002). Intercellular communication across gap junctions influences a wide range of cellular and tissue activities, including regulation of growth, differentiation, and developmental signalling (Willecke et al. 1991). Gap junctional intercellular communication (GJIC) is known to be a general mechanism for achieving rapid syncitial communication within a tissue including the spread of electrical waves in cardiac tissue (Kimura et al. 1995, Severs et al. 1999). Gap junctions are also present in the nervous system where they coordinate synchronous neuronal firing and switching between neuronal

pathways. In non-excitable, differentiated but avascular tissues, GJIC allows passage of nutrients, e.g. in the eye lens (Simon et al. 1998). GJIC takes part in controlling cell proliferation and differentiation in various tissues, and it is influenced, in turn, by the cell-cycle (Loewenstein et al. 1992, Kamei et al. 2003).

The first connexin to be expressed in the embryo, and one of the best-studied, is known as Cx43. Neuronal progenitors in the developing mouse cerebral cortex require Cx43-mediated coupling to keep them in a self-renewing state, and differentiate prematurely or die when it is inhibited (Cheng et al. 2004). Cx43 is also required for normal cell proliferation in the developing chick eye (Becker et al. 1999). Also, Cx43 gap junction assembly in the mouse begins during compaction in the 8-cell stage (Becker et al. 1995) and could prepare the implanting conceptus for rapid diversification of cell types during gastrulation in preimplantation development (Kidder et al. 2001). The importance of gap junction communication can also be assessed in different human diseases associated with the lack of properly functioning connexins. The first disease shown to result from connexion mutation in is a form of Charcot-Marie-Tooth disease (CMT). Point mutation of Cx32 gene causes progressive neurodegeneration due to Schwann cell disfunction in CMT (Bergoffen et al. 1993). Also, the Nonsyndromic Deafness, one of the most prevalent inherited sensory disorders among children is caused by the mutation of Cx26 (Mignon et al. 1996).

Gap junctions in skeletal muscle differentiation

Detection of gap junction structures in muscle development

Gap junctions are found in most solid tissues with the notable exception of adult skeletal muscle (Dermietzel 1990) which is understandable, because myofibers are multinucleated syncitia where no membrane borders can be found. In differentiated muscle, connexins are mainly restricted to the vascular endothelia (Araya et al. 2005) and to the smooth muscle and stromal cells producing Cx43 type gap junctions.

During skeletal muscle development an ultrasructural analysis demonstrated the presence of gap junction like structures for the first time in freeze fracture replicas of fetal rat muscles (Rash and Staehelin 1974) and between interacting myoblasts in developing chick muscle (9-day-old embryo) as small plaques of tightly packed particles (Kalderon et al. 1977). Similar studies showed adhering junction plaques between primary myotubes and inserting secondary myotubes in rat embryos (Duxson et al. 1989). At birth, skeletal muscle of newborn rats are still immature, and ultrastructural analysis can reveal gap junction structures between

postnatal myofibers, but one week after birth no gap junctions are found anymore (Schmalbruch et al. 1982).

Transient connexin expression in skeletal muscle development

Subunits of gap junction channels are the connexin proteins, which are encoded by a gene family consisting of at least 20 genes in humans and 19 in the mouse (Willecke et al. 2002). Different types of connexin proteins have been identified during early skeletal muscle development, and various connexion subtypes have been detected in different animal species. However, the expression of connexin isotypes was transient and restricted mainly to the embryonic phase. Cx40 was found transiently expressed in axial skeletal muscle of mouse embryos (Dahl et al. 1995), but it was not detected in adult muscle regeneration (Araya et al. 2005). Recently, Cx39 was identified with northern blot and PCR analysis in skeletal muscle of mouse embryos between the embryonic day 13.5 and birth, but it was absent from the adult animal. Punctate immunofluorescence signals of Cx39 were prominent in different muscles of the mouse embryo, (Maltzahn et al. 2003) but interestingly no other connexin type was found in that study. In regenerating muscle precursors derived from postnatal mice, both Cx43 and Cx45 were upregulated, but only Cx43 seemed to play a prominent role in normal regenerative myogenesis (Araya et al. 2005). Cx43 and 45 were also expressed in satellite cell-derived primary myoblast cultures and functional coupling could be detected at both 24 and 48 hours of culture (Araya et al. 2005)

Functional gap junction communication and its possible role in embryonic myogenesis

First functional studies, in relation to the possible involvement of gap junctions in early skeletal muscle development were done in transformed myogenic cell lines, which tumor cells, however do not represent all features of *in vivo* myogenic cells. Cx43 was detected *in vitro* in prefusion myoblasts using C2C12 cell line (Constantin and Cronier 2000). Also, Cx43 was found to be expressed in cycling L6 myoblast cell line, and dye transfer experiments, in which small molecular weight fluorescent dye can pass through gap junctions, showed functional coupling at early stage of culturing these cells (Balogh et al. 1993). The functional coupling detected in the L6 cell line, could be reversibly inhibited using gap junction blockers 18-α-glycerrhetinic acid or octanol, which also downregulated myogenin expression and myotube formation (Proulx et al. 1997). However, these and other chemical gap junction blockers are not specific and have many side effects. In primary myoblast cultures of rats, cell to cell dye diffusion was restricted to a short prefusion lag period, and disappeared during

fusion promotion. However, dye diffusion was sometimes observed between myoblasts and newly formed myotubes too. Another study also confirmed that the gap junction blocker heptanol reduced the formation of multinucleated myotubes (Constantin et al. 1997). Furthermore, the inducible deletion of Cx43 in mice myoblasts resulted in the inhibition of dye-coupling and the delayed expression of the muscle differentiation marker, myogenin (Araya et al. 2005).

All these findings suggested that gap junction communication is transiently involved at the prefusion lag period of early skeletal muscle development, but no comprehensive study was done to dissect the temporal regulation of gap junction connexin expression and coupling in the course of myogenic progenitor cells differentiating into multinucleate myofibers. Despite the evidence that disruption of GJIC results in delay of muscle development, the precise mechanism and timing of its action during early myogenic development and interactions with other regulatory factors are yet to be clarified.

Aim of this study

The aim of this study was to determine the spatio-temporal regulation of gap junction connexin expression and function during early myogenic differentiation, and see how these affect myoblast proliferation and fusion using both *in vivo* and *in vitro* rat models. Ultrastructural, immunomorphological, and functional dye transfer techniqes were utilized in combination with laser scanning microscopy, quantitative image analysis and gene transfection studies.

1) Notexin induced muscle regeneration model recapitulating *in vivo* myogenesis was used to study the spatio-temporal expression of gap junction Cx isoforms during myoblast differentiation and fusion in correlation with factors of cell proliferation (Ki67) and cell cycle control ($p21^{waf1/Cip1}$ $p27^{kip1}$).

2) Primary myoblast cultures set up from muscle precursor cells of the same species used for the regeneration model were applied to study the temporal correlation of Cx expression and functional dye coupling through Cx43 gap junctions, with particular attention to the prefusion period, using quantitative data analysis.

3) Primary myoblast cultures also, were used to manipulate Cx43 expression and function using gene transfection with wild-type or dominant-negative eGFP (enhanced green protein)-Cx43 vector constructs, as well as an eGFP-only control (wtCx43, dnCx43 or GFP-only). Functional changes of up- and downregulated gap junction coupling were correlated with myoblast differentiation and fusion.

Materials and Methods

In vivo muscle regeneration

Notexin induced regeneration

Muscle regeneration was induced in adult Wistar rats according to a standard protocol from our laboratory (Zador et al. 1996). Briefly, anaesthetized male rats (5 mg pentobarbital sodium (Nembutal)/100g body weight) of ~350g were injected with notexin, the venom of a mainland tiger snake (Notechis scutatus scutatus; Sigma), into the soleus muscle of their left legs after gently pulling aside the gastrocnemius muscle through a small incision. Twenty μg notexin, dissolved in 200 μl sterile saline was introduced into the middle part of the muscle sack and then the wound was closed with a suture. The soleus muscle of the right leg was injected with saline alone to serve as a control. The middle one-third of the soleus muscle was excised on days 1,2,3,4,5 and 7 after notexin administration, at least 3 animals were studied in each group. Additional 2 animals were sacrificed at days 21 and 28 of the regeneration, respectively. Tissues were processed for morphological and immunohistochemical analysis. The animals were housed in pairs, and provided with normal laboratory food and water supply at libitum. Animal experiments were performed in accordance with the Animal (Scientific) Act 1986 of the UK and were approved by the Ethical Committee of the University of Szeged.

Semithin resin sections and electron microscopy

Small pieces (2x1x1 mm) of the muscles were fixed in 2% glutaraldehyde, postfixed in 4% osmium tetroxide and contrasted en block with 1% uranyl acetate. Fixed tissues were dehydrated in graded ethanol series and embedded from propylene oxide into TAAB 812 (TAAB Laboratories Equipment Ltd) epoxy resin. Semithin resin sections (1μm thick) were cut with ultramicrotome and stained with methylene blue and basic fuchsine for light microscopic analysis. Representative resin-embedded blocks were selected, trimmed and ultrathin sections of 80-100 nm thin were cut for electron microscopy and studied with a JEOL JM 1010 instrument.

Immunostaining for connexin isotypes

Different connexin isotypes were analysed both on sections of regenerated muscles and on adherent primary myoblast cultures. Table 1 summarizes connexin antibodies used in this study.

Connexin	Epitope sequence residues	Dilution	Animal source	Designation/ Clone	Reference/supplier
Cx26	Proprietary sequence of intracellular loop of rat Cx26	1:100	Mouse	Monoclonal CX-12H10	Zhang and Nicholson 1989 Zymed Lab. (San Francisco, CA)
	106-119 of intracellular loop of rat Cx26	1:300	Rabbit	Polyclonal Des 3	Becker et al. (1995), kind gift from Prof. H. Evans
Cx32	Proprietary sequence of intracellular loop of rat Cx32	1:100	Mouse	Monoclonal CX-2C2	Milks et al. 1988 Zymed Lab.
	108-119 of intracellular loop of rat Cx26	1:300	Rabbit	Polyclonal Des5	Boitano et al. 1998, kind gift from Prof. H. Evans
Cx37	266-281 of cytoplasmic C terminal of rat Cx37	1:100	Rabbit	Polyclonal Y16Y/R4	Yeh et al. 1998, kind gift from Prof. N. Severs
Cx40	254-268 of cytoplasmic C terminal of rat Cx40	1:500	Rabbit	Polyclonal	Yeh et al. 1997, kind gift from Dr. R.G. Gourdie
Cx43	Proprietary sequence of cytoplasmic C terminal of rat Cx43	1:200	Mouse	Monoclonal CX-1B1	Krenacs et al. 1997 Zymed Lab.
	131-142 of intracellular loop of rat Cx43	1:200	Mouse	Monoclonal Gap 1A	Wright et al. 2001
	131-142 of intracellular loop of rat Cx43	1:300	Rabbit	Polyclonal Gap15	Becker et al 1995
Cx45		1:100	Rabbit	Polyclonal B2/1895	Becker
	354-367 of cytoplasmic C terminal of rat Cx43	1:100	Guinea pig	Polyclonal	Coppen et al. 1998, kind gift from Prof. N. Severs

Table 1. Anti connexin antibodies

Immunostaining of sections for single and double antigens

One of the muscle samples was snap-frozen in isopentane cooled liquid nitrogen and the other was fixed in 4% formaldehyde and embedded routinely in paraffin wax. Cryostat sections of 6 μm thick were cut from the frozen samples, which were mounted on charged glass slides (SuperFrost Plus), then fixed in acetone for 5 minutes and air dried at room temperature for 30 minutes before immunostaining. Paraffin sections of 4 μm thick were immunostained after a wet-heat induced epitope retrieval procedure by cooking of dewaxed sections in a 0.1 M Tris - 0,01 M EDTA solution (pH 9.0) at 120 °C for 2 min 30 sec in a Tefal Clipso pressure cooker (Krenacs et al. 1999). Sections were rinsed in TBS (Tris-buffered saline) pH 7.2 and blocked with a solution containing 1% BSA (bovine serum albumin) and 0,1% sodium azide in TBS, for 15 minutes. The same solution was used for diluting all immunoreagents except the fluorescent or peroxidase labelled ones, which were diluted in neat TBS. Sections for immunoperoxidase staining were also pre-treated with a 1.5% hydrogen peroxide methanol solution for blocking endogenous peroxidases. The

following antibodies were used for immunostaining frozen sections: monoclonal mouse anti-desmin (clone: D33, 1:200; or clone DE-R-11, 1:20) -muscle specific actin (clone: HHF35, 1:50), -myo-D1 (clone: 5.8A, NovoCastra; 1:50), polyclonal rabbit anti-chicken desmin (1:200); and different type of anti-connexin antibodies (Table 1). Paraffin sections were immunostained for desmin (D33, see above), -p21$^{waf1/Cip1}$ (clone: SX118), -p27^{kip1} (clone:SX53G8; both 1:100), and rabbit polyclonal Ki67 (Mib-1, 1:500). The sections were incubated with the primary antibodies in humidified chambers at room temperature for 2h. Then washed three times in TBS before using either biotinylated anti-rabbit or anti-mouse immunoglobulins (Igs, 1:150) for frozen sections, or peroxidase-conjugated anti-mouse or anti-rabbit EnVision$^+$ reagents (1:200) for paraffin sections, for 40 minutes. In case of double labeling, secondary reagents were also applied simultaneously by mixing either biotinylated goat anti-mouse Igs (1:150) with rhodamin labelled anti-rabbit Igs (1:100), or biotinylated anti-rabbit Igs (1:150) with rhodamin labelled anti-mouse Igs (1:100). After washing 3 times in TBS, frozen sections were further incubated with FITC-streptavidin (1:200) for another 30 minutes. All immunoreagents were from DakoCytomation, except where otherwise indicated. All sections were mounted without dehydration with Faramount medium (DakoCytomation). Sections stained for immunofluorescence were examined with a Leica TCS SP confocal laser-scanning microscope (Leica) using 1024x1024 pixels resolution either in single or dual channel (FITC/TRITC) modes.

Quantitative image analysis of Cx43 and cell cycle associated proteins

The levels of Cx43 expression and the percentage of myogenic cell nuclei immunopositive for the cell cycle associated p21$^{waf1/Cip1}$, p27^{kip1} and Ki67 proteins were analyzed on digital images at each stage. For Cx43, 2 frozen sections of 6 µm thickness were cut at standard orientation from different levels of the treated muscles of 3 animals every stage. Standard magnification (x20), gain and pinhole settings of the confocal microscope were used to achieve the best possible signal-to-noise ratio. At least two representative images were collected on each muscle sample making up 6-8 images per stage. Digital single channels images were transformed into 8 bit black-and-white format and were analyzed using the ImageJ 1.29x software (Wayne Rasband, NIH, USA). At standard threshold settings, which ensured that only specific signals were considered and the background was excluded, the area fraction of Cx43 immunofluorescent plaques was measured on each image. The means of percentages in each group were summarized in graphs. Statistical analysis included

the calculations of standard error and the significance of difference between various stages using the paired Student t-test.

The 3 paraffin blocks collected every stage were cut 5µm thick serial sections, immunostained for desmin, $p21^{waf1/Cip1}$, $p27^{kip1}$ and Ki67, respectively and counterstained with hematoxylin and eosin. Myogenic cells were recognized by their characteristic morphology confirmed by desmin immunopositivity. Series of digital images were collected on the immunostained samples using a transmission light microscope at x20 magnification fosucing on representative areas where degenerating and regenerating muscles were longitudinally oriented. The expression of cell cycle associated molecules by myogenic cells was characterized by calculating the percentage of immunopositive myogenic cell nuclei of all myonuclei found on the particular image. The mean values and standard error of means were summarized in a graph.

Primary myoblast culture

Isolation and culturing newborn rat myoblasts

The cultures were set up using a modified protocol of that published earlier by our laboratory (Keresztes 1991). Briefly, excised muscle samples were collected in phosphate buffered saline pH 7,2 (PBS) before being cut into small pieces (2-3 mm) and placed in PBS in eppendorf tubes. Muscle samples were treated with 0.25% trypsin (4 U/mg, Serva Feinbiochemica) dissolved in PBS, and shaken for 30 min, after which the supernatants were collected. Trypsin was added to the pellet and the digestion continued for another 30 minutes. Supernatants from both fractions were mixed and pipetted into clean eppendorf tubes and centrifuged twice in PBS at 2000 rpm for 10 min. All steps were performed at room temperature. The supernatants were discarded and the cell pellets resuspended in complete Dulbecco's MEM growth medium containing 10% fetal calf serum, 10% horse serum and 200 µg/ml Gentamycin (all reagents were from Sigma). Pre-plating of the cells in growth medium using macroplates at 37 °C for 25 min was applied to eliminate fibroblasts. The cell density of the supernatant was adjusted to $2x10^5$ cells/well and incubated in 24 well plates at 37 °C, in 5% CO_2. Cells were grown on coverslips coated with 2 mg/ml poly-L-lysine (Sigma) and 1,5 µg/ml laminin (Sigma) and the growth medium was changed daily. Coverslips were examined daily to count transfected cells, or removed for immunostaining or functional dye-transfer testing. Fusion index was calculated in percentage on standard x40 confocal images by counting cell nuclei, counterstained with 7-amino-actinomycine D (7-AAD, 1:1000, Molecular Probes Inc), in myotubes, divided by the number of all nuclei in the field and

multiplied by 100, in desmin immunostained cultures. The mean values calculated by using 10 images from 3 different series of cultures at each stage were summarized in a graph.

Immunostaining of myoblast cultures

Cultures on coverslips at different stages of their development (1–8 days) were rinsed twice with PBS and fixed in fresh acetone for 5 min. After drying at room temperature for 30 min they were rinsed in PBS and blocked with 1% L-lysine (Sigma) in PBS for 15 min. Incubation with primary antibodies was carried out at room temperature for 1.5 h in a humidified chamber. The following primary antibodies were used, diluted in the blocking solution: anti-desmin, anti-Cx43 (Gap1A, Gap15, see Table 1). Cultures were washed in PBS three times for 5 min and incubated with the secondary antibodies, diluted in PBS, for 40 min. Secondary antibodies for single and double labelling were combinations of goat anti-mouse or goat anti-rabbit Alexa Fluor 488 (Molecular Probes: Invitrogen; 1:500) and goat anti-mouse or goat anti-rabbit Cy3 (Zymed; 1:500). For nuclear counterstaining, bisbenzimide (Hoechst 33258, Sigma; 1:1000) was applied in the first of 3x5-min PBS washes. Cultures were mounted using Citifluor AF1 antifade mountant (Citifluor Ltd.), and the coverslip edges sealed with nail varnish. Images of immunostained samples were captured using the same confocal laser scanning microscope as previously.

Image analysis of Cx43 immunofluorescence in differentiating myoblasts

Connexin43 protein expression was also analyzed quantitatively during the differentiation process. At least 3 cultures on coverslip were immunostained for Cx43 each day between day-1 and day-5 of differentiation and 8-10 representative images per stage were captured and analysed with the Image J softver. Standard 1024x1024 pixel x20 images of 300 dpi resolutions were used for image analysis. Particles were counted at 3 different size ranges, representing all particles (5-2500 pixel range), dot-like particles of ≤1 μm (5-80 pixel range) mostly confined to cell membranes, and large intracytoplasmic plaques of ≥4μm (320-2500 pixel range) of Cx43, respectively.

Transfection of adherent myoblasts

Two days after plating, adherent primary myoblast cultures were transfected with pIRES2-eGFP vectors (Biosciences Clontech) containing sequences coding for eGFP alone, eGFP and wild-type Cx43 (wtCx43), or eGFP and a dominant-negative, C-terminal-truncated, trafficking-impaired modification of Cx43 in which the valine at position 231 is converted to glutamic acid and a termination codon occurs after the phenylalanine at position 232

(dnCx43) (Becker et al. 2001). Transfection was performed at about ~30% confluence using Effectene™ transfection reagent (Qiagen, Crawley, UK) according to the manufacturer's instructions. In brief, for each well of the 24-well plate, 1 µl of the appropriate construct (1µg/ml) was prepared by mixing with 150 µl of kit buffer and 8 µl of enhancer, and incubated for 2–3 min at room temperature in an Eppendorf tube. Then 25 µl of Effectene™ reagent was added to this , mixed again and incubated for 5–10 min at room temperature. The culture was washed twice with fresh PBS and returned to growth medium (1 ml) and the entire transfection mixture was added dropwise to the well. Transfected cultures were incubated for 24 h, and then returned to normal growth medium. Cultures were transfected at day 2, and the green fluorescence of eGFP could be seen within 5–6 hours. The incidence of transfection and the behaviour of the cells were monitored for 1–4 days after tranfection (3–6 day-old cultures). Coverslips were transferred into Krebs solution and examined with a fluorescence microscope using a x20 water immersion objective (Leica HCX), and images were captured using a digital camera (Leica DC 300FL). Consistency of transfection was checked by treating 12 parallel cultures using the pIRES2-eGFP vector alone (GFP-only). Green-fluorescing GFP$^+$ cells were monitored on days 1, 2, 3, 4 after transfection and counted in images taken from 21 non-overlapping random fields of view on each coverslip, each with an area of 0.094 mm^2. Cultures were counterstained with bisbenzimide (1:1000) so that the total number of nuclei in each field of view could also be counted. Subsequent transfection of cultures with the GFP-only, wtCx43 and dnCx43 constructs were performed in parallel on four coverslips for each construct, and monitored in the same way. For each coverslip, the total number of GFP$^+$ cells and the total number of bisbenzimide-labelled nuclei in the field of view were recorded on each day after transfection, plotted and statistically analysed. In the early stages of culture, all GFP$^+$ cells contained one nucleus but at later stages, multinucleated myotubes were also present, and these were counted independently. Consistency of transfection across the coverslips and the significanceof the effects of any treatment were tested using Kruskal-Wallis one-way ANOVA by ranks calculations, followed by pairwise inter-group comparisons performed with the Dunn's method (SigmaStat, Sigma). For brevity, we refer to this combination of non-parametric methods as the KWD test.

Dye transfer assays

Dye coupling of myoblasts through gap junctions was studied with two microinjection assays. Either the gap junction permeant Lucifer Yellow CH (Mr 457 Da) alone or the combination of the gap junction impermeant Dextran-Fluorescein (Dextran-FITC; Mr 10

kDa) and the junction permeant Cascade Blue analogue 8-methoxypyrene-1,3,6-trisulfonic acid trisodium salt (MPTS; Mr 538 Da) (all from Molecular Probes Inc.) tracers were used as earlier (Becker et al. 1995). Samples of myoblast cultures grown on coverslips were taken out daily between day-1 and day-5 of normal cultures or 3-6 days after transfection, and placed into fresh medium using 30mm microplates fixed on the stage of an epifluorescence microscope. Glass microelectrodes were filled either with a 5% Lucifer Yellow CH, or a mixture of 5% MPTS and 10mg/ml dextran-fluorescein solutions and backfilled with 1M/l buffered (pH7.2) lithium chloride. Microelectrodes were introduced into the cytoplasm of myoblasts under visual control and small pulses of negative current were used to ionophorese the dye(s) into the cells. The spread of fluorescent tracers was visualized under epifluorescence illumination using either blue (435 nm) or green (520 nm) emission filters and images were captured after 3 min with a CCD camera. Combined phase-contrast and fluorescent images of each area were also collected. At least 10 different cells were microinjected with each tracer on each coverslip, and at least 2 coverslips were subjected to dye microinjection at each time point. The efficiency of myoblast dye coupling in non-manipulated cultures was calculated based on counting coupled per injected cells as revealed on digital images. To exclude cytoplasmic bridges of early myoblast fusion from the study, only those coupling events were considered where the dextran tracer did not pass to any adjacent cell. In case of transfection studies, a junctional coupling index was calculated as the number of adjacent myoblasts showing Cascade Blue fluorescence, but not dextran-FITC fluorescence, per injected cell; and the cytoplasmic coupling index was assessed from the number of neighbours showing FITC fluorescence, per injected cell.

Results

Localizing connexins and gap junctions in rat skeletal muscle

Mature muscle contains stromal fibroblasts and endothelial cells known also to express connexins, thus identification of muscle cells was crucial in this study. Desmin was found as a very early marker of muscle cell differentiation consistently detected throughout the whole spectrum of muscle cells including early myoblasts (muscle precursors) of round or unipolar shapes (Fig. 4A-B), and thus it was used to identify muscle cells throughout regeneration and in primary myoblast cultures.
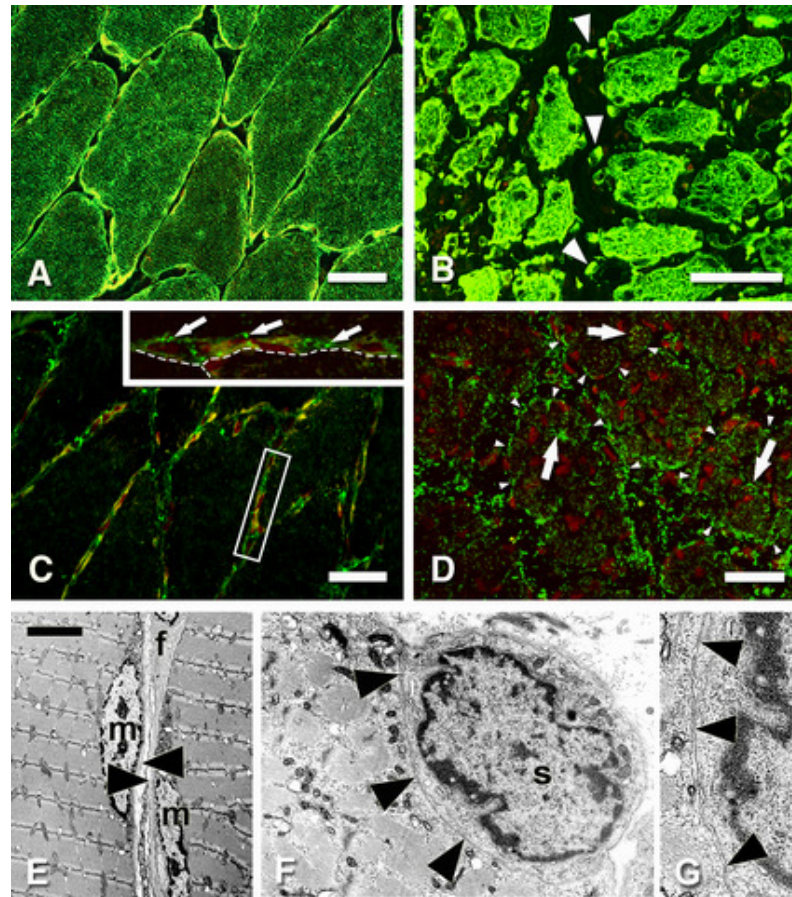
Figure 4. Detection of desmin, and Cx43 gap junctions in rat soleus muscle.
(A) Sensitive immunostaining of desmin intermediate filaments in intact myofibers (B) Desmin in early myoblasts (arrowheads) of notexin-induced day-2 muscle regeneration (C) Rare Cx43 immunoreactivity (green, arrows) of stromal and endothelial cells in the extracellular space D) In newborn muscle Cx43 (green) is detected both along (arrowheads) and inside (arrows) immature fibres bearing many internal myonuclei (red). (E) Mature muscle myofibers are separated by basal lamina (arrowheads). (F-G) There is no close membrane apposition, between a satellite cell (s) and an adjacent muscle fiber (arrowheads). m = myonucleus, f = fibroblast. Immunofluorescence based confocal laser scanning microscopy (CLSM) in frozen sections, cell nuclei are stained red with 7-AAD (A-D), and electron microscopy (EM) (E and F). Bars: A-D = 30 µm; Bar on E: E = 3 µm; F = 800 nm; G = 400 nm.

In intact skeletal muscle and in notexin-induced muscle regeneration six connexin isotypes were tested (26, -32, -37, -40, -43 and -Cx45), and only Cx43 showed reliable immunoreaction on desmin positive myogenic cells as compared to control samples. In mature skeletal muscle some Cx43 was detected in vascular endothelial cells accompanied with Cx37 and/or Cx40, and in endomyseal stromal cells but not in desmin positive muscle fibers (Fig. 4C). Immature muscle fibers of newborn rats, however, showed some Cx43 immunostaining inside fibres (Fig. 4D). Sarcolemmae of adjacent mature fibers were separated by thin basal laminae preventing direct cell-to-cell contacts (Fig. 6E). Also, there were no ultrastructural signs of gap junctions between the cell membranes of mature muscle fibers and resting satellite cells (Fig. 4F-G).

Gap junctions in notexin-treated soleus muscle

Early regeneration

Signs of acute, necrotizing tissue damage were detected within a few hours after notexin injection. Neutrophil granulocytes and then histiocytes invaded the muscle and extracellular edema was obvious (Fig. 5A). Swollen muscle fibers with fragmented and dissolving cytoskeletal structures and many activated macrophages were enveloped by basal lamina (Fig. 5B). Few myoblasts were detected and parcially all were in the cell cycle as characterized by strong nuclear Ki67 staining and no positivity for $p21^{waf1}$ and $p27^{kip1}$ reactions. Connexin43 immunostaining was limited at this stage and it was also confined to the myoblasts along pre-existing muscle fibers (Fig. 5C). Despite the massive myonecrosis, only some diffuse, extracellular desmin reaction indicated the damage of endomyseal basal lamina at the molecular level.

Upregulation of Cx43 protein in invading myoblasts prior fusion

After 48h, extensive phagocytosis of tissue debris by macrophages was accompanied by massive myoblast invasion (Fig. 5D). Edema became more pronounced and desmin positive myoblast, spindle-shaped cells usually with prominent nucleoli and basophilic cytoplasms, were apparent at large numbers (Fig. 5E). Some were clearly dividing but most were bipolar and seemed to interact with each other. They gathered along the pre-existing muscle fibers and produced significant amount of punctuate Cx43 staining as they did so (Fig. 5F). Only weak $p21^{waf1}$ and $p27^{kip1}$ nuclear immunostaining could be detected in less than 30% of them. At the same time, nearly 90% of myoblasts strongly expressed the proliferation associated Ki67 nuclear protein. Ultrastructural hallmarks of gap junctions, close membrane appositions were also found between a few adjacent myoblasts (Figs 5G-H). Double immunolabeling co-localized Cx43 and desmin in myogenic cells (Fig. 5I). Inflammatory cells invading the damaged fibers did not show immunodetectable Cx43.

Upregulation of $p21^{waf1/Cip1}$ and $p27^{kip1}$ expression in aligned myoblasts

Three days (72 h) after notexin administration large numbers of myoblasts were aligned with close membrane apposition along the pre-existing basal lamina and the number of inflammatory cells were reduced (Fig. 6A). Some groups of aligned myoblasts already started to fuse and form multinucleate myotubes.
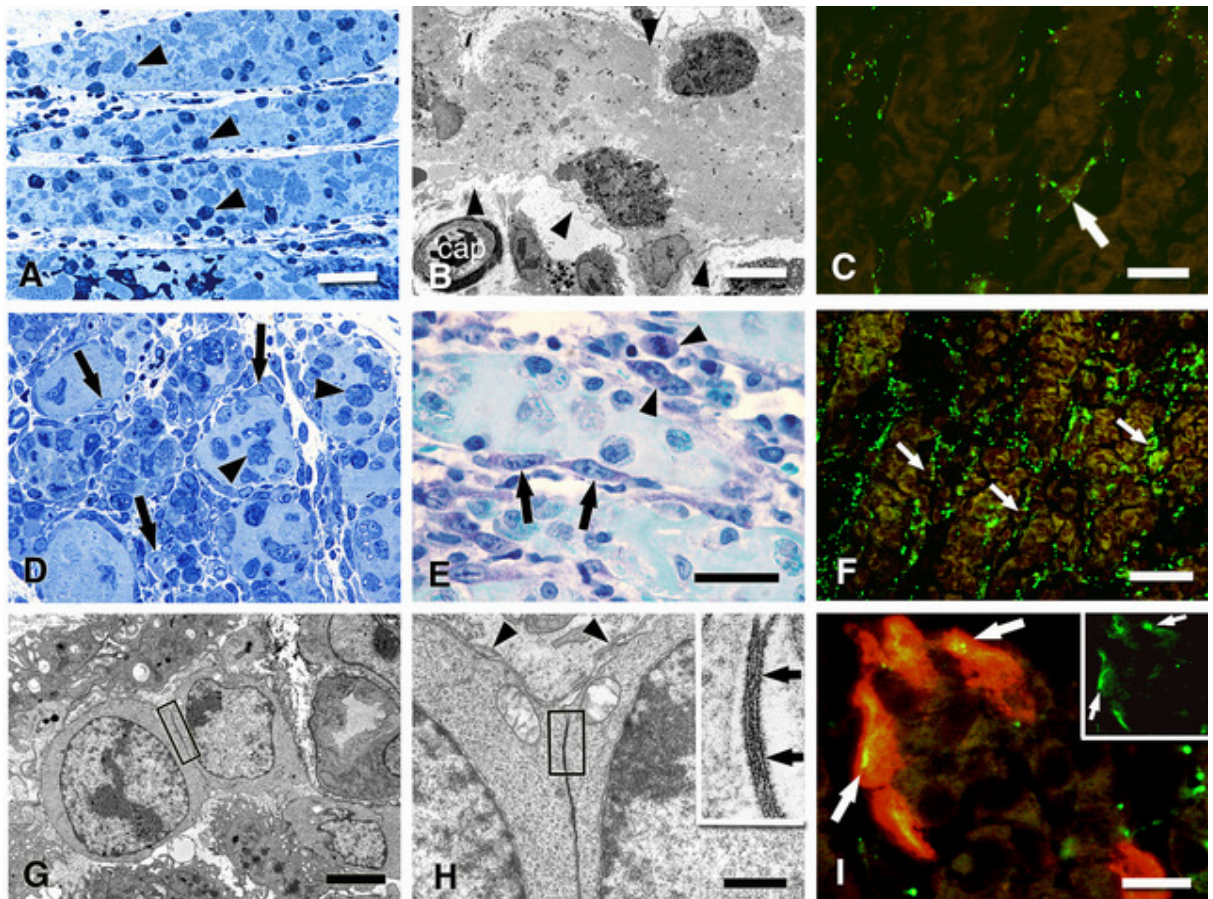
Figure 5. Notexin-induced muscle regeneration/differentiation
Day-1: A) Damaged muscle fibres are infiltrated by macrophages (arrowheads) and neutrophils. B) Basal laminae (arrowheads) and blood capillaries (cap) are preserved. C) The amount of Cx43 protein (green) is low, but it is detected on an early myoblast (arrow).
Day-2: D) Myoblasts (arrows) and activated phagocytes (arrowheads) in a cross section. E) Bipolar myogenic cells (arrows), some of them are dividing (arrowheads), are associated with the pre-existing fibres. F) Elevated amounts of Cx43 (green) are in overlapping location with the invading myoblasts (arrows). G-H) Close membrane appositions (rectangles and arrows in the inset) suggestive of gap junctions are between adjacent myoblasts I) Co-expression of Cx43 (green) and desmin (red) in myoblasts is shown in yellow (arrows)
Methylene blue-basic fuchsine (MB-BF) stained semithin resin sections (A, D, E), CLSM in frozen sections (C, F, I) and EM (G, H). Bars: A, D=25 µm; B=7 µm; C, E= 5 µm; F = 35 µm; G = 4 µm; H=600 nm (inset = 80 nm); I = 10 µm (inset = 20 µm).

The peak of myoblast invasion was accompanied with the highest amount of Cx43 detected (Fig. 6B), mainly along myoblasts (Fig. 6C). By this stage, the majority of aligned myoblast showed massive expression of p21[waf1/Cip1] (Fig. 6D) and p27[kip1] (Fig. 6E) while lacking the proliferation marker Ki67 (Fig. 6F), which indicated their synchronized exit from the cell cycle.
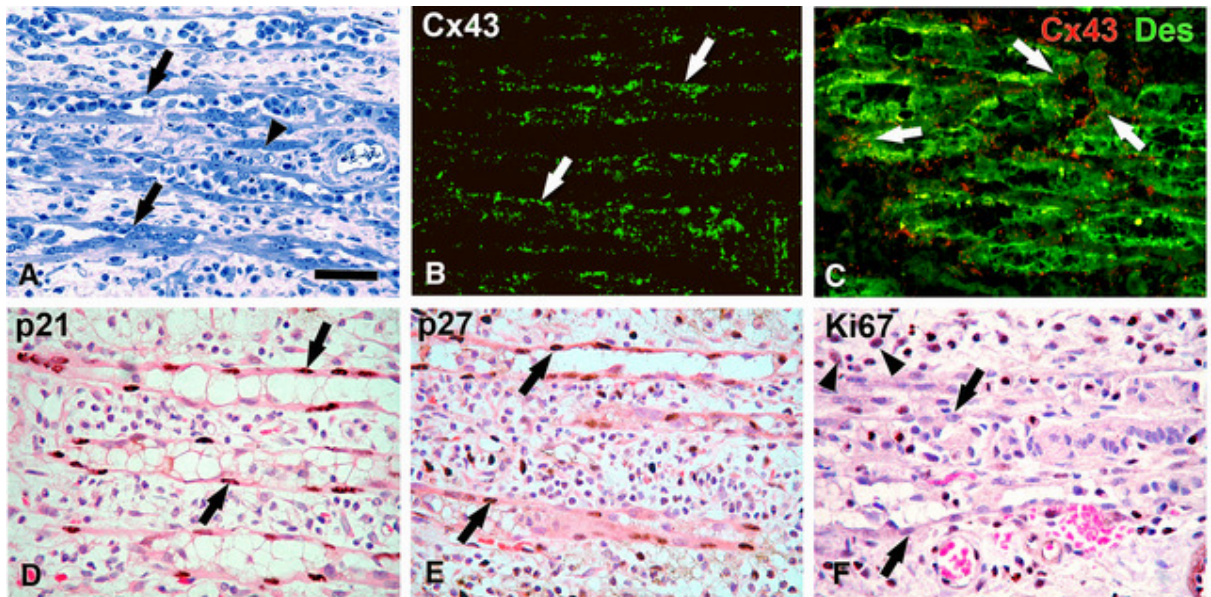
Figure 6. Notexin-induced muscle regeneration/differentiation, day-3
A) Alignment (arrows) and fusion (arrowheads) of myoblasts in a central area of massive tissue damage full of inflammatory cells. B) Large amounts of Cx43 protein along the myogenic cells (green; arrows). C) Connexin43 (red) is co-expressed with desmin (green) in the myogenic cells (arrows). Strong nuclear expression of cyclin dependent kinase inhibitor proteins p21$^{waf1/Cip1}$ (D) and p27^{kip1} (E). F) Single myoblasts are still in the cell cycle (Ki67; arrowheads), while aligned myoblasts stopped proliferating as indicated by the missing Ki67 nuclear staining (arrows). MB-BF stained semithin resin section (A), immunofluorescence and CLSM in frozen sections (B, C), and immunoperoxidase reactions (brown) counterstained with H&E in paraffin-embedded sections (D, E, F). Bar: 35 µm.

Diminishing of connexin43 protein after myoblast fusion

By day-4 of regeneration, edema and the number of phagocytic cells was further reduced. Myoblast alignment was clearly visible with most of the completed fusion and newly formed myotubes started to produce bundles of contractile elements. Connexin43 protein expression rapidly declined with the progression of myoblast fusion into syncytial myotubes.

At this stage of regeneration mononucleate myoblasts were still present and expressed Cx43. Both cell cycle control proteins p21$^{waf1/Cip1}$ and p27^{kip1} were detected in large numbers of myonuclei. Then p21$^{waf1/Cip1}$ was reduced during further maturation, while p27^{kip1} was still detected in most cell nuclei of myofibers. There was no considerable change in Cx43 expression of the desmin negative areas during the regeneration process.

During early stages of regeneration, both Cx43 and cell cycle associated molecules expressed by myoblasts were quantitatively analysed and summarized in Figs. 7A and 7B. Myogenic cell nuclei including single, aligned and fused cells were all considered at counting immunopositive cells, except those of degenerating myofibres on day-1.
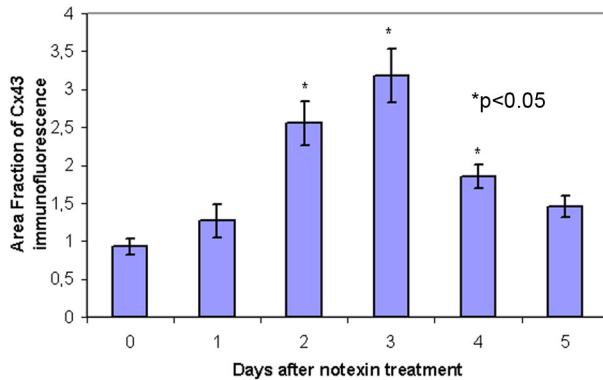
Figure 7A. Image analysis of Cx43 protein expression in regenerating rat soleus muscle. Summary of means of area fraction of Cx43 expression. There is a significant elevation in gap junction protein levels (* p< 0,05) between days 2-4 after notexin treatment as probed with the t-test. Myoblast fusion started on day-3. Standard error = ⊥.
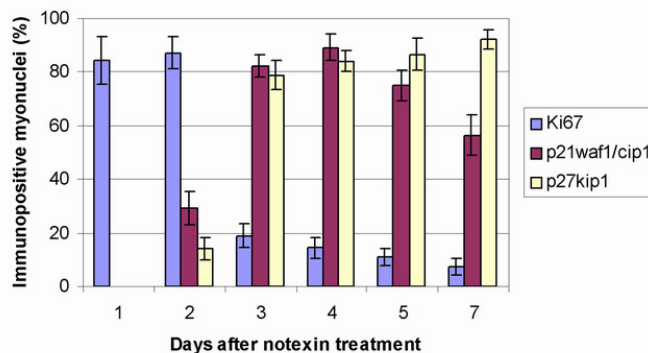
Figure 7B. Expression of cell cycle associated proteins by myogenic cells in regenerating rat soleus muscle. On day-1, most myoblasts were positive for the proliferation marker Ki67 but all were negative for p21[waf1/Cip1], p27[kip1] cyclin dependent kinase inhibitors. In all other stages myonuclei of single aligned and fused cells were considered. Standard error = ⊥.

By day-7, newly formed muscle fibers showed conspicuous bundles of contractile elements, but their nuclei were randomly arranged and their sarcoplasms vacuolated. Regenerated fibers showed intensive desmin expression but only very rare Cx43 staining. The regeneration process was completed between days 21-28, by which time muscle morphology and Cx43 expression of regenerated fibers did not differ considerably from those in control muscles. Only the central position and high density of cell nuclei in some muscle fibers reflected the former regeneration.

Gap junctions in differentiating non-manipulated primary myoblast culture

Upregulation of Cx43 expression before myoblast fusion

Similarly to our *in vitro* model, myoblasts were identified with desmin immunostaining to exclude non-muscle cells from the study. Same set of Cx isotypes were tested in rat primary myoblasts including Cx26, -32, -37, -45 (not shown) and Cx40 (Fig. 8D), and Cx43. Cx43 was only detectable, which is line with our findings in regenerating skeletal muscle. Over 90% of cultured cells were desmin positive (Fig. 8A).

In day-1 cultures, myoblasts have rounded or slightly elongated shape and started to express Cx43 protein (Fig. 8B-C). Double immunolabeling for Cx43 and desmin confirmed

cell membrane-bound and cytoplasmic Cx43 not only in cells of physical contacts with each other, but also in non-interacting myoblasts.

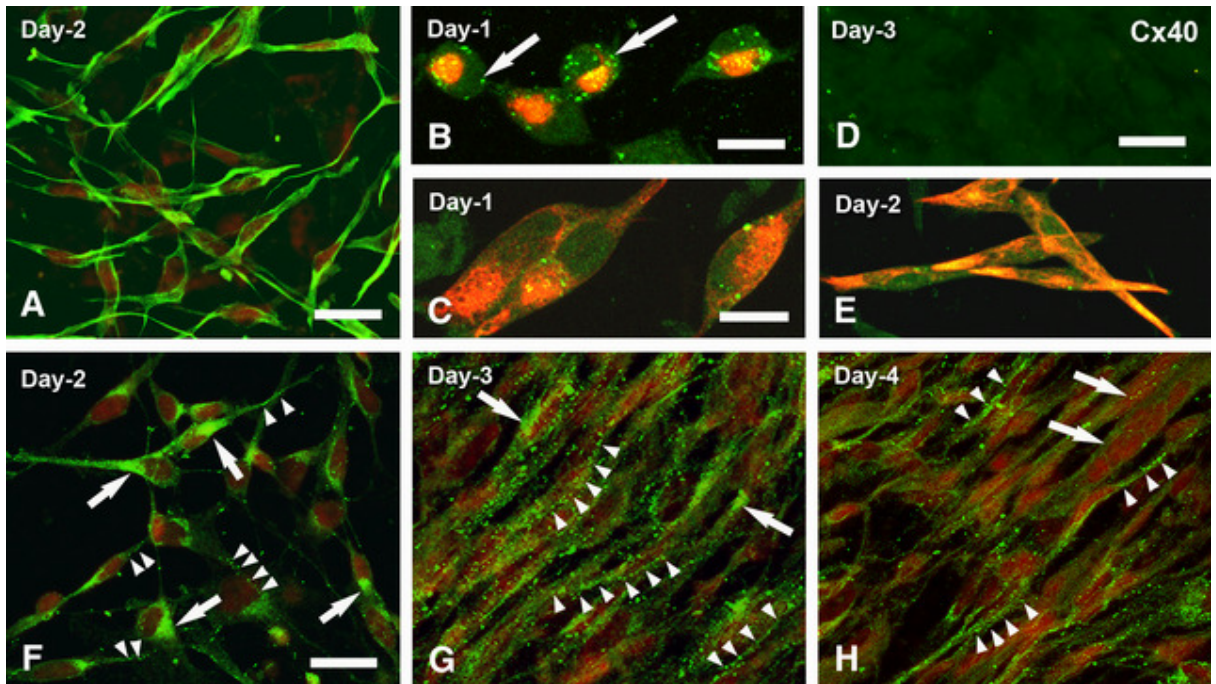**Figure 8.** Cx43 protein expression in differentiating primary myoblasts
A) Desmin immunostaining confirms myogenic origin of the cells in a day-2 culture. Punctuate Cx43 (green dots) appears early in desmin positive (red) myoblasts of round (B) or slightly elongated shapes (C) in day-1 cultures. Single myoblasts express Cx43 without contacting neighbors (arrows). D) Confluent day-3 myoblasts show no specific immunostaining for Cx40. E) Myoblasts co-localizing Cx43 (green) and desmin (red) in yellow in a day-2 culture. F) Day-2 myoblasts is featured by granular paranuclear immunoreactions (arrows) and cell membrane associated single particles (arrowheads). G) Day-3 confluent myoblasts are aligned and express high numbers of particulate signals in their cell membranes (arrowheads) and less significant cytoplasmic (arrows) Cx43. H) In day-4 culture, multinucleate myotubes (arrows) hold only little immunoreaction, while mononucleate myoblasts still produce much cell membrane associated Cx43 (arrowheads). Cell nuclei are stained red with 7-AAD except on B-E. Double immunolabeling using polyclonal anti-Cx43 (Gap 15, green) and monoclonal anti-desmin (D33, red) antibodies (B, C, E). Immunofluorescence based CLSM. Bars: A = 15 µm; B = 6 µm; C = 4-µm; F = 8 µm; D, E = 15 µm; F-H = 10 µm.

By day-2, cultures were still sparse, but elongated and spindle shaped myoblasts were linked to their neighbors (see Fig. 8A). Double labeling proved Cx43 and desmin co-localization in them (Fig. 8E). Connexin43 protein expression was greatly upregulated as compared to that of day-1 cultures (Fig. 8F). Cx43 was detected as dotlike signal along myoblast membranes and massive granular immunostaining in their paranuclear region reflecting extensive production and assembly of gap junction channels. There was no sign of cell fusion at this stage. By day-3, most contacting myoblasts were aligned in the confluent areas. Membrane associated Cx43 particles increased substantially, while the cytoplasmic fraction significantly reduced (Fig. 8G), as compared to those on day-2 (see Fig 8F). Rarely, bi- or trinucleate cells appeared reflecting the start of myoblast fusion at this stage. The peak

of Cx43 expression was detected on the 2nd and 3rd day of regeneration but it was linked with diverse subcellular distribution.

By day-4, numerous multinucleate myotubes were formed bearing strong desmin reaction. Cx43 immunostaining was restricted to mononucleate myoblasts and only very few signals were detected in myotubes (Fig. 8H) similar to that we observed in regeneration. By days 5-6 of differentiation, the majority of myoblasts formed multinucleate myotubes with only rare and small patches of Cx43 protein. By day-7, large myotubes and increasing numbers of dying myogenic cells were seen. The fusion index is summarized in Fig. 9.
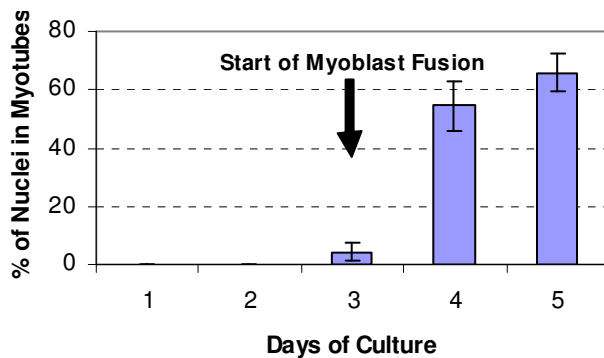
Figure 9.
A) Fusion index shows % of myonuclei found in myotubes. Myoblast fusion started on day-3.

Quantitative image analysis of Cx43 expression data was also done in immunostained myoblast cultures. Our main purpose was to clearly separate cell membrane particles of Cx43 immunostaining from the large cytoplasmic plaques using image segmentation based on signal intensity and size. Using this approach, high levels of Cx43 protein were detected on day-2 and day-3, which were significantly higher than those found at earlier or later stages. However, the number of small, cell membrane-associated particles (size range 5-80 pixels) was significantly increased by day-3 on the expense of the intracytoplasmic clusters (size range 320-2500 pixels), as compared to that of the day-2 stage (data are not shown).

Upregulation of dye coupling in randomly arranged myoblasts followed by a downregulation before fusion

In primary myoblast cultures Lucifer Yellow alone was microinjected into single cells that were in contact with their neighbors. Some myotubes were also targeted. To exclude possible fusing cells from the study, injections were not considered if Lucifer Yellow spread instantly. Coupling was considered successful when dye spread into 2 or more cells. The efficiency of cell coupling was calculated based on coupled per injected cells.

In sparse day-1 cultures, the communicating cells were coupled to 1-2 neighbors most they were in contact with (Fig. 10A-B). Significant elevation in cell coupling was found in

day-2 cultures, where the dye frequently passed into several cells in the 2nd and 3rd order from the injected myoblast (Fig. 10C-D). Day-3 cultures were still coupled but less myoblasts were involved than in day-2 cultures and permeability of Cx43 channels became significantly reduced between day-2 and day-3 preceding syncytial membrane fusion (Fig. 10E). The coupling frequency declined further by day-4 and at later stages upon progression of myoblast fusion and the appearance of increased numbers of myotubes (Fig. 10F-G). Primary myotubes were coupled only to some neighbouring myoblasts (Fig. 10H-I), and rare coupling events were also seen between adjacent early myotubes (Fig. 10J).
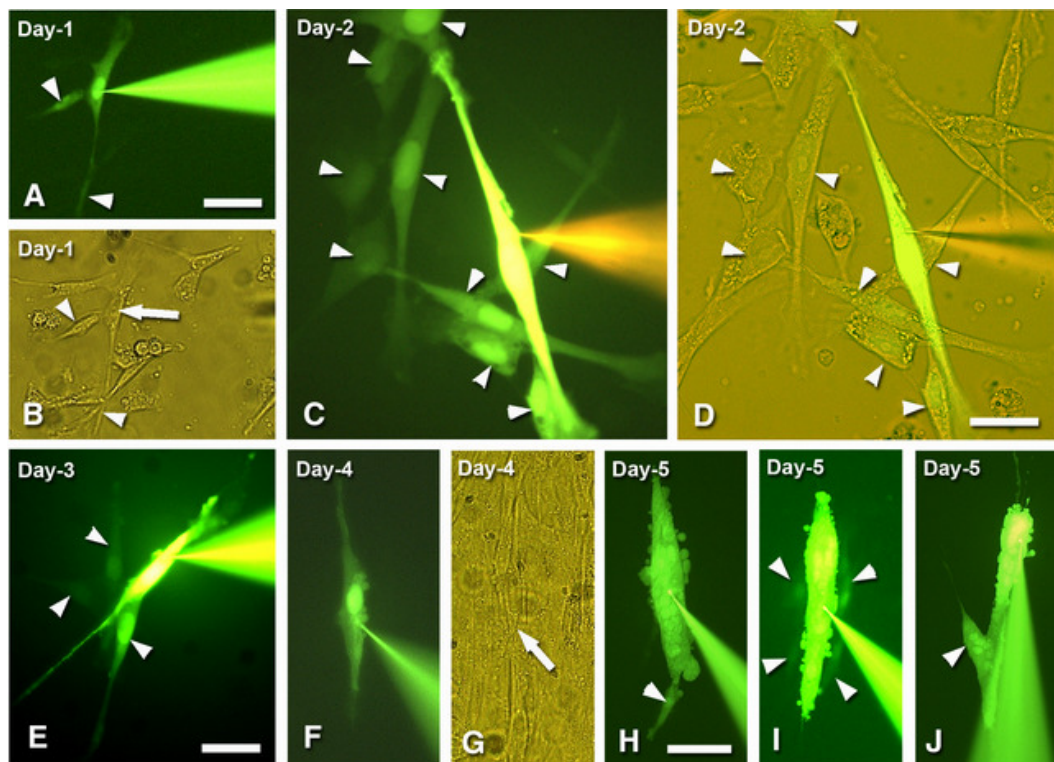
Figure 10. Lucifer yellow dye transfer assay of gap junction coupling in primary myoblast culture, coupled cells are labeled with arrowheads. Epifluorescence (A, C, E, F, H, I, J) and phase contrast (B, D, G) images. Dye coupling in a sparse day-1 culture (A, B). Highly efficient coupling involves almost all cells on the imaged area in a day-2 culture (C, D). Day-3 culture is still coupled (E), however, there is no coupling in a confluent day-4 culture containing multinucleate myotubes (F, G). Rare coupling events are seen between myotubes and adjacent myoblasts (H, I), and between early myotubes (J) in day-5 cultures. Arrows point to the entry of dye injection on B and G. Bars: A, B = 15 µm; C,D = 8 µm; E-G = 10 µm; H-J = 25 µm.

Gap junctions in manipulated primary myoblast cultures

GFP expression in transfected myoblast cultures

To determine the contribution of Cx43-mediated gap-junctional communication to myoblast proliferation, differentiation and fusion into myotubes, we manipulated the expression of Cx43 in myoblast cultures. Transfection of adherent myoblast cultures on the 2nd day of culture, prior to the normal peak of cell membrane associated Cx43 protein under

these conditions, was performed with pIRES2-eGFP, either alone (GFP-only) or containing wild-type Cx43 (wtCx43) or a dominant-negative gene construct (dnCx43). To demonstrate the consistency of transfection, we analysed 12 parallel cultures, all treated with pIRES2-eGFP construct alone. Following transfection, cultures were monitored for 4 days and fluorescence images of GFP and a nuclear stain (bisbenzimide) were taken from 21 random fields of view in each culture at each stage (Fig 11A). GFP$^+$ cell number, total cell (nuclear) number, the ratio of GFP$^+$ cells to cell nuclei and GFP$^+$ myotubes (tubes were detectable at day 5 and 6 of culturing) were followed and analysed. Transfection was found to be consistent in parallel cultures one day after transfection and the ratio of GFP$^+$ cells to cell nuclei declined at later stages as expression of the pIRES-eGFP construct was always transient (graphs are not shown).

Effects of modified Cx43 expression on cell numbers and myotube formation

Our main aim in this study was to examine the effects on myoblast numbers and myotube formation of modifying the connexin content of the myoblasts, either by overexpressing the wild-type Cx43 sequence or by expressing a well-characterized dominant-negative version that disrupts junctional communication. Four coverslips treated with each construct were examined on each day after transfection. Consistency of transfection was also achieved when parallel cultures were treated with the GFP-only, wtCx43 or dnCx43 constructs and they were compared one day after transfection (Fig 11B)
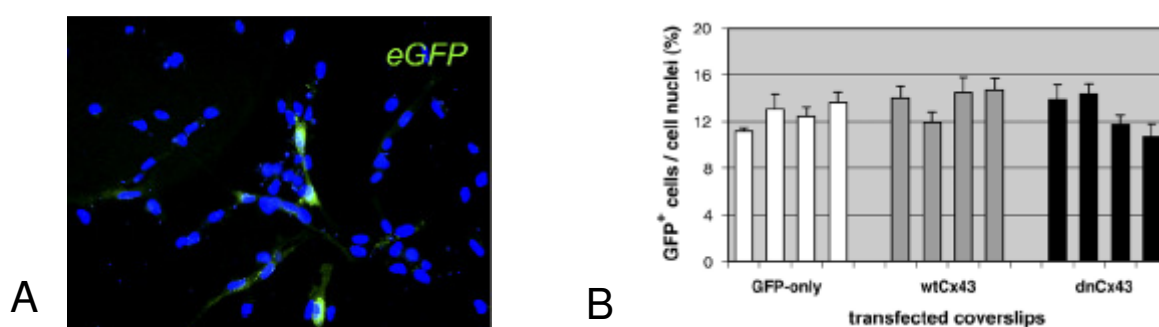
Figure 11.
A) Primary myoblast culture, 3 days after plating and 1 day after transfection with pIRES-eGFP (green). Ten cells in this field (typically 12% of the total) are GFP+.
B) Ratios of mean GFP$^+$ myoblast numbers to total cell numbers, one day after transfection of four coverslips with each of the three pIRES constructs.

Two days after transfection, the numbers of GFP$^+$ cells and the total cell number had risen in all groups, indicating that transfected and untransfected cells had all continued to proliferate. GFP-only and wtCx43-transfected cells showed similar, moderate increases, but dnCx43-transfected cells showed significantly larger increases (dnCx43 vs GFP-only,

p<0.001; dnCx43 vs wtCx43, p<0.001) with typically twice as many GFP$^+$ cells per field of view (Fig. 12A). The increase in total nuclear count per field of view in the dnCx43-transfected cultures was smaller in proportion than the increase in GFP$^+$ cells, but greater in absolute terms, and was also significant (dnCx43 vs GFP-only, p<0.05; dnCx43 vs wtCx43, p<0.05).
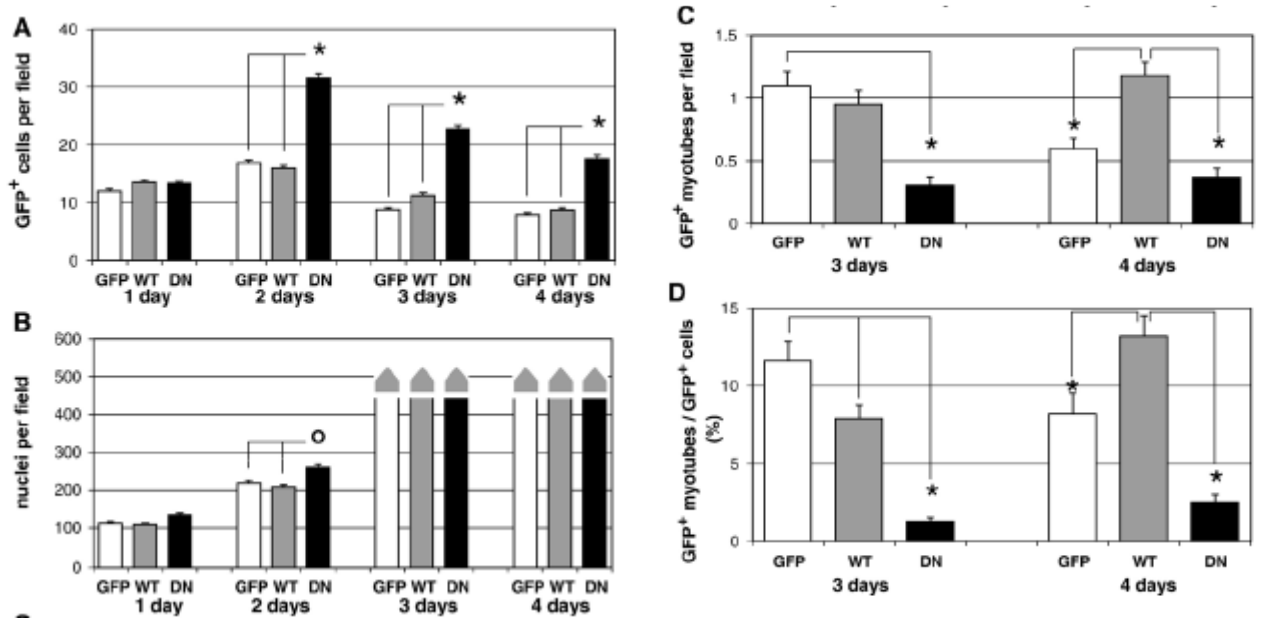
Figure 12.
A. Mean numbers of GFP$^+$ myoblasts per field for 21 non-overlapping fields in each of four parallel coverslip cultures, recorded for four days after transfection with each of the three pIRES constructs (GFP = GFP-only; WT = wtCx43; DN = dnCx43).
B. Mean numbers of nuclei per field for the same cultures. From three days after transfection onwards, nuclei overlapped too much to be counted accurately.
C, D: Mean numbers of GFP$^+$ myotubes (C) and ratios of GFP$^+$ myotubes to all GFP$^+$ cell outlines (D), for the same cultures.
Error bars in all parts represent SEMs. Asterisks mark differences at the p<0.001 level by the Kruskal-Wallis ANOVA with Dunn's method of inter-group comparison. The circle in B marks a difference at the p<0.05 level.

Three days after transfection, the number of GFP$^+$ cells had declined by about half in the GFP-only and wtCx43 groups. However, the number of GFP$^+$ cells had declined much less in the dnCx43 group, remaining significantly higher than in the other two groups (dnCx43 vs GFP-only or wtCx43, p<0.001) (Fig. 12A). Myotubes were already present in significant numbers in the GFP-only and wtCx43 cultures at this stage, which explains part of the difference in GFP$^+$ cell numbers among these groups (Fig. 12C; dnCx43 vs GFP-only, p<0.001) Ratio of myotubes to mononucleate GFP$^+$ cells differed even more between the three treatments (Fig. 12D). Both the higher counts of mononucleate cells and the lower

counts of myotubes in the dnCx43 cultures at this stage may reflect the extent to which dnCx43-transfected myoblasts had failed to fuse into myotubes, as well as possible sustained differences in proliferation. In all treatment groups at this stage, the total number of bisbenzimide-stained nuclei per field was too high to be recorded with accuracy because of cell and nuclear overlap (Fig. 12B) and significant differences between the treatment groups in this respect were no longer detectable. Four days after transfection, the number of GFP$^+$ cells in each treatment group (including GFP$^+$ myotubes, each counted as one cell) had continued to decline a little, but the number in the dnCx43 group remained significantly higher (approximately double that in the other groups: dnCx43 vs GFP-only or wtCx43, p<0.001, Fig. 12A). At this stage, significantly more GFP$^+$ myotubes could be detected in wtCx43 cultures than in either GFP-only or dnCx43 cultures (wtCx43 > GFP-only > dnCx43; wtCx43 vs GFP-only p<0.001, dnCx43 vs GFP-only, p<0.001; Fig. 12C).

In summary, cells over-expressing wtCx43 were seen to form as many GFP$^+$ myotubes as cells transfected with GFP only, and appeared to maintain them in the GFP$^+$ state for longer. In contrast, cells transfected with the communication-impairing dnCx43 construct increased their numbers much more than those in either of the other groups during the pre-fusion period, up to two days after transfection, and most of them remained in a potentially proliferative, unfused state thereafter. Such cells were found in large numbers as GFP$^+$ mononucleate cells throughout the experiment, and were significantly retarded in myotube formation.

Effects of modified Cx43 expression on intercellular coupling

Dye coupling tests combining the gap junction permeable Cascade Blue analogue and the channel-impermeable Dextran-fluorescein (can pass only when cytoplasmic continuities are present) was applied in non-manipulated primary myoblast cultures first, and resulted in similar data to those gained with the Lucifer Yellow assay. The efficiency of dye coupling in differentiating primary myoblast cultures was measured by calculating coupled per injected cells as it is summarized in Fig. 13. It had to be noted that in aligned day-3 myoblasts double of the concentration of membrane-bound Cx43 was found to mediate only half as efficient dye coupling than in those of randomly arranged day-2 myoblasts. This suggested that the permeability of Cx43 channels became significantly reduced between day-2 and day-3 preceding syncytial membrane fusion.

The incidence and pattern of coupling among neighbouring cells in each transfected groups was examined using the same combination of Cascade Blue with FITC-dextran. Examples of how the junctional and cytoplasmic types of coupling can be distinguished using

these dyes. To obtain an overview of the coupling patterns, each injected cell was assigned to one of four classes: no coupling, exclusively junctional coupling, junctional coupling to at least one neighbour and cytoplasmic coupling to at least one other neighbour (mixed coupling), or exclusively cytoplasmic coupling (Fig. 14A). The differences in incidence of these four coupling patterns between the three treatments, pooled across time, were found to be very highly significant (p<0.0001; chi-squared test; n=181).
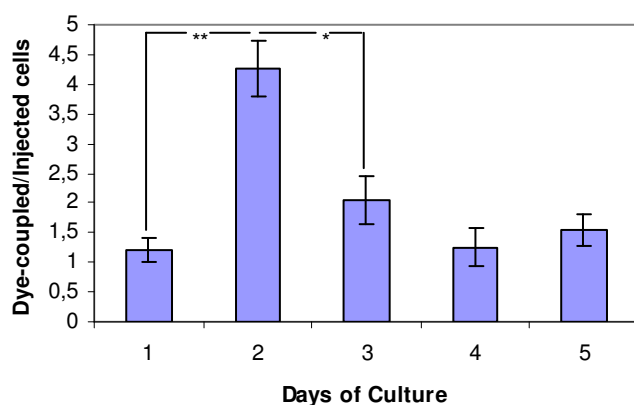
Figure 13. Efficiency of dye coupling in differentiating primary myoblasts demonstrating the means of coupled per injected cells. There is a significant peak of myoblast coupling on day-2 (***p< 0,01*) compared to all other stages. The difference between day-2 and day-3 is still significant (**p< 0,05*). Standard error = ⊥.

One day after transfection, in the GFP-only treatment group 72% of GFP^{+} cells showed coupling, which is characteristic of three-day-old proliferating myoblast cultures, and 16% were cytoplasmically coupled. GFP^{+} cells in the wtCx43 group showed an even higher total incidence of coupling, reaching 90%, and cytoplasmic coupling to 37%. The presence of cytoplasmic coupling suggests the possibility of excess early cell-fusion events in this group. However, no overt fusion into myotubes was observed at this stage. GFP^{+} cells in the dnCx43 group showed a significantly reduced overall coupling incidence of 36%, all of which was junctional coupling (for all coupling: GFP-only vs dnCx43, p≤0.005; wtCx43 vs dnCx43, p≤0.002). One-and-a-half days after transfection, the overall coupling level in the GFP-only group was barely changed (71%) with 50% cytoplasmic coupling. All of the injected wtCx43 cells were coupled, and 90% (9/10) were coupled cytoplasmically to at least one other cell. In extreme contrast, the overall incidence of coupling in the dnCx43 group was only 30% (3/10), and only 10% (1/10) of dnCx43 cells were coupled cytoplasmically (all coupling: GFP-only vs dnCx43, p≤0.025, wtCx43 vs dnCx43, p≤0.004).

Two days after transfection, the total incidence of coupling in injected GFP-only cells had decreased to 50%, and cytoplasmic coupling (including mixed cases) had fallen to 28%. In contrast, all wtCx43 cells were still coupled (78% cytoplasmically). In the dnCx43 group, the total incidence of coupling had risen to 44% and that of cytoplasmic coupling to 19%, but the wtCx43 cells remained significantly more highly coupled (all coupling: GFP-only vs wtCx43,

p=0.0001; wtCx43 vs dnCx43, p=0.0001). Three days after transfection, the total incidence of coupling in the GFP-only group was 44% (all junctional). Among wtCx43 cells, overall coupling remained high (86%) with 14% showed mixed coupling and 22% showing exclusively cytoplasmic coupling. By contrast, in the dnCx43 group, the total incidence of coupling had fallen to 25% (4/16) and, just as in the GFP-only group (all junctional). As at previous time-points, these differences were statistically significant (all coupling: GFP-only vs wtCx43, p=0.008; wtCx43 vs dnCx43, p=0.001).

Fig. 14B shows junctional-coupling indices at each time point for the neighbours of injected cells transfected by each of the three treatments, and Fig. 14C shows the corresponding cytoplasmic-coupling indices. In summary, wtCx43 cells, which would be expected to have more functional gap junctions than the other groups, did indeed show higher levels of junctional coupling; but they also showed cytoplasmic coupling both earlier and more extensively than the other groups, consistent with precocious entry into the early stages of cell fusion. Conversely, in dnCx43 cells, our coupling data not only showed that the presence of the dominant-negative connexin reduced gap-junctional communication at all stages, as expected, but also that its presence almost eliminated cytoplasmic coupling, reinforcing our morphological observation that dnCx43 cells were retarded in cell fusion.
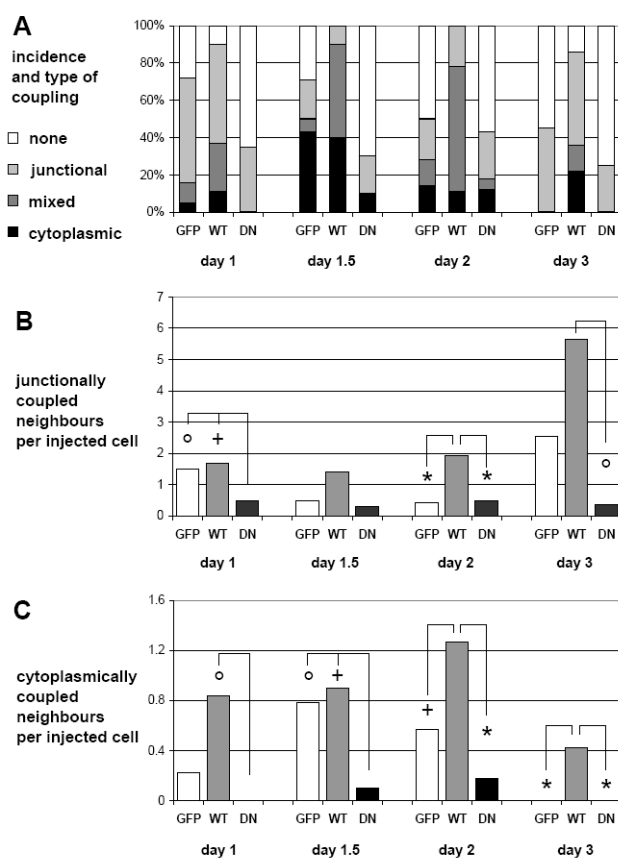
Figure 14.
A. Outcomes of Cascade Blue/FITC-dextran injections into GFP$^+$ cells. Type of coupling was classified into junctional, mixed and cytoplasmic coupling.
B. Junctional coupling indices. Cells contributing to this chart received Cascade Blue, but not FITC-dextran, from their injected neighbour. Gap-junctional coupling was present throughout the experiment in all treatment groups, but was strongest after wtCx43 transfection and weakest after dnCx43 transfection, as would be expected.
C. Cytoplasmic coupling indices. Cells contributing to this chart received both Cascade Blue and FITC-dextran from their injected neighbour. Cytoplasmic coupling peaked in all groups on the third or fourth day after plating, 1.5-2 days after transfection, but it was consistently commonest after wtCx43 transfection and rarest after dnCx43 transfection.
For individual days in B and C: asterisk: $p<=0.0025$; plus: $p<=0.01$; circle: $p<=0.025$.

Discussion

Expression of Cx isotypes in early myogenesis

By testing for six connexins, we found only Cx43 in regenerating rat soleus muscle and primary myoblasts, the isotype, which was detected by most research groups in vertebrate myogenic cells either in tissues or in cell cultures. It should be noted, that some connexins have orthologues in other species with different molecular masses (Willecke et al. 2002). In the chick, Cx36 and -42 and -45 were found in the myotome and/or the dermomyotome of somites (Berthoud et al. 2004) and Cx43 in the pectoral muscle of the embryo (Beyer 1990). In the mouse, Cx39 (von Maltzahn et al. 2004) and Cx40 (Dahl et al. 1995) were described in embryonic myotubes, while Cx43 and -45 were detected in adult muscle regeneration (Araya et al. 2005).

We analysed muscle sections and myoblast cultures of rats with parallel immunostainings, using purified mono- and polyclonal antibodies for some Cx-s. Double labeling with desmin and Cx43 showed that gap junctions were expressed by myogenic cells. This direct evidence was missing from earlier works (Mege et al. 1994; Constantin et al. 1997; Constantin and Cronier 2000) though it would have been was crucial throughout, since other cell types with similar morphology such as stromal fibroblasts and endothelial cells also express this type of Cx (Ko et al. 2000; Liao et al. 2001). Our negative finding of Cx32 is in line with an earlier study not detecting this Cx in L6 myogenic cells (Balogh et al. 1993). However, our missing evidence for Cx40 contradicts with that published by Dahl et al. (1995) in 16,5 days mouse embryo. Interestingly, Cx43 was not detected in their model, which either suggests that there might be a switch between Cx isotypes during muscle development, or Cx gene expression may differ between mice and rats. This idea is further supported, by the finding of Cx45 in transgenic mice muscles (Araya et al. 2005) and by the detection of Cx39 exclusively in developing mouse muscles between embryonic day 13.5 and birth (von Maltzahn et al. 2004). Myogenic cell lines of rat (L6) (Balogh et al. 1993) or murine (C2C12) (Constantin and Cronier, 2000) origin are also restricted to form Cx43 channels only. However, the results on transformed cell lines must be handled cautiously, due to the altered phenotype and gene expression profile of cell lines compared to primary myoblasts. For instance, L6 cells are deficient in producing adequate amount of MyoD transcripts (Proulx et al. 1997), and C2 cells may become tumorigenic at transplantation (Rando and Blau, 1994). Nevertheless, these data suggest that more than one Cx isotype is involved during early muscle differentiation in vertebrates and Cx43 channels seems to be dominating.

Main findings on gap junctional intercellular communication during early myogenesis

Formation of gap junctions is a ubiquitous feature of cells devoted to multicellular functions (Kumar and Gilula 1996). Several studies have detected gap junctions (Kalderon et al. 1977; Rash and Fambrough 1973; Schmalbruch et al. 1982), connexins and/or cell coupling in myogenic cells before fusion and the downregulation of these features in multinucleate myotubes (reviewed by Constantin and Cronier, 2000). However, the way, as gap-junctional coupling influences muscle development (Araya et al. 2005; Constantin et al. 1997; Mege et al. 1994; Proulx et al. 1997), myoblast proliferation, differentiation and fusion still needed further clarification.

In this study, we provide *in vivo* and *in vitro* evidence on the transient expression and developmental regulation of gap junction connexins in differentiating myoblasts preceding fusion during notexin-induced muscle regeneration in adult rats and in primary myoblast cultures originated from newborn rats, respectively. In both experimental systems Cx43 was the exclusive gap junction isoprotein expressed by desmin positive myogenic cells. Cx43 appeared early in proliferating single myogenic cells, followed by a progressive upregulation in the cytoplasmic and cell-membrane domains of interacting myoblasts until fusion and then by a rapid fall in multinucleate myotubes. In regeneration, elevated production of Cx43 channels in aligned prefusion myoblasts was accompanied by the widespread nuclear expression of cyclin dependent kinase inhibitor proteins $p21^{waf1/Cip1}$ and $p27^{kip1}$ and the complete loss of the proliferation associated Ki67 protein suggesting a synchronized exit of cell cycle before fusion and a potential role of gap junction coupling in regulating these processes. In myoblast cultures, the temporal regulation of dye coupling, reflecting direct cell-cell communication was correlated with connexin expression. Extensive dye coupling in sparse meshworks of myoblasts with relatively few cell membrane connexin channels was followed by a decline of coupling in aligned, still prefusion cells despite enhanced cell membrane Cx43 expression. Both coupling and Cx43 expression were significantly reduced in confluent post-fusion cultures rich in primary myotubes.

In searching for further functional evidenve, Cx43 expression of early myoblasts was manipulated by transfecting them with wild-type or dominant-negative eGFP-Cx43 constructs, or with an eGFP-only control. Myoblasts transfected with wtCx43 showed more gap-junctional coupling than GFP-only controls, began fusion sooner as judged by the incidence of cytoplasmic coupling, and formed more myotubes. DnCx43 transfected cultures remained proliferative for longer than either GFP-only or wtCx43 myoblasts, showed less

coupling, and underwent little fusion into myotubes. All of our above findings suggest that Cx43 gap junctions are involved in the regulation of cell cycle control in aligned prefusion myoblasts, which could contribute to synchronizing myoblast differentiation for a coordinated syncytial fusion.

Transient involvement of gap junction communication in early skeletal muscle differentiation

Muscle regeneration after myotoxic injury has been thoroughly studied by our group (Zador et al. 1996) and served as our *in vivo* model of muscle development. Similar to previous reports, the venom of the Tiger snake called notexin, causes a selective myonecrosis accompanied by excessive inflammation and fast repair of the muscle (Harris et al. 1975; Lefaucheur and Sebille 1995). Regeneration recapitulates ontogenic muscle differentiation including the activation and myogenic commitment of stem cells, followed by their proliferation, interactions, cell cycle exit, alignment and fusion into multinucleate myotubes (Constantin and Cronier 2000). At the beginning of regeneration, the mitogens released from damaged myofibers activate satellite cells, whereas inflammation-derived growth factors maintain their cell cycle progression (Bischoff et al. 1990).

Quiescent satellite cells did not express Cx43 protein, but presumptive myoblasts produced connexins as early as they appeared. The membrane-bound Cx43 in non-interacting myoblasts may represent gap junction hemichannels, which are regulated in the same way as the aligned channels (Goodenough and Paul 2003). Very early gap junction formation has also been suggested in cultured chick myoblasts based on preserved ionic coupling despite blocking of protein synthesis 16h after myoblast plating (Kalderon et al. 1977). The short half-life of Cx43 protein, about 1.5-2h, allows gap junctions to form and adapt rapidly to changing physiological demands (Beardslee et al. 1998). We found that myoblast invasion and alignment were proportional to the range of inflammation and macrophage infiltration. Unlike in some papers, we, however, did not find immunodetectable connexins in the inflammatory cells during muscle regeneration (Alves et al. 1996; Eugenin et al. 2003). Macrophage-secreted factors have been shown to enhance proliferation, chemotactic migration and differentiation of myoblasts and to be essential for the growth of transplanted myogenic cells (Cantini et al. 2002; Lescaudron et al. 1999; Robertson et al. 1993). Concurrent with this finding, macrophage infiltration has dramatically increased Cx43 mRNA and protein levels in mesenchymal cells on day-3 in a nerve crush injury (Chandross et al. 1996). Desmin negative stromal cells also express Cx43 protein (Ko et al. 2000), therefore,

transient communication between myoblasts and stromal cells through homotypic Cx43 channels may not be excluded.

The pattern of Cx43 expression and phenotypic myoblast maturation detected in primary myoblast cultures was found to be highly comparable in regenerating muscles and in primary cultures of the same animal species. Our functional data showed that direct cell-cell communication through gap junctions was most active in the proliferating, sparse meshworks of myoblasts and the efficiency of myoblast coupling became significantly downregulated in the aligned, still prefuion but postmitotic cells. A role for the downregulated gap junction communication in the initiation of myoblast fusion may not be excluded too. Several studies showed transient involvement of Cx43 gap junction before primary myotube formation, but these works did not distinguish the mitotic and postmitotic stages of prefusion myoblasts differentiation and showed no clear indication of the timing of fusion (Araya et al. 2005, Constantin et al. 1997). Other studies have gained controversial results using transformed myogenic cells lines to experience e.g. the complete disappearance and reappearance of the Cx43 protein (Balogh et al. 1993), or used the inaccurate scrape-loading dye coupling test (Mege et al. 1994). For these reasons, we focused our attention on correlating the regulation of gap junction expression and cell coupling in prefusion primary myoblasts, which also form normal muscle *in vivo*.

Cx expression and control of cell cycle in early muscle regeneration

Membrane associated gap junctions are transiently expressed by proliferating and differentiating myoblasts, thus information exchange via these channels could have direct effect during early stages of myogenesis. To participate in the large-scale fusion within a short-time-frame as it happens normally, a multitude of proliferating myoblasts must leave the cell cycle synchronously and escape apoptosis. Cyclin dependent kinase inhibitors including $p21^{waf1/Cip1}$ and $p27^{kip1}$ (Sherr and Roberts 1999; Walsh and Perlman 1997) control this event and thus they may play key roles in the growth arrest and survival of proliferating myoblasts (Kitzmann and Fernandez 2001; Ostrovsky and Bengal 2003). $p21^{waf1/Cip1}$ can be activated through either MyoD dependent or independent pathways (Lawlor and Rotwein 2000; Walsh and Perlman 1997). Enforced Cx43 expression causes the elevation of $p27^{kip1}$ in tumor cell lines resulting in the inhibition of cell cycle transition from G1 to S phase and a subsequent growth arrest (Koffer et al. 2000). We detected evenly high levels of both $p21^{waf1/Cip1}$ and $p27^{kip1}$ proteins in the nuclei of aligned myoblasts just preceding fusion, following the general upregulation of Cx43 gap junctions. At the same time, all aligned myoblasts lost the

proliferation associated Ki67 protein confirming their synchronized exit from the cell cycle. Furthermore, Cx43 gap junctions can activate p21$^{waf1/Cip1}$ in bystander cells (Azzam et al. 2001). Thus, Cx43 channels in prefusion myoblasts could be involved in the regulation of cell cycle control either directly or through a bystander transactivation mechanism. This would be a feasible pathway for synchronizing myoblast differentiation for the rapid and large-scale fusion (Rash and Fambrough 1973).

Gap junction coupling between myoblasts *in vitro*

Intracellular injection and cell-to-cell spreading of a gap-junction-permeant dye such as Lucifer Yellow is an established technique for assessing functional gap-junction coupling. This technique was applied in maturing primary myoblast cultures to monitor temporal regulation of gap-junction coupling in correlation with connexin expression. Most extensive dye transfer was found in sparse, day 2 cultures, which result was confirmed by combining the gap junction permeant Cascade Blue, mixed with a non-permeant fluorescent dextran, to distinguish junctional coupling from dye spread through cytoplasmic continuities (Bukauskas et al. 1992; Pearson et al. 2004). In many studies of coupling during myogenesis, communication has been assessed using only a single gap-junction-permeant dye without a gap-junction-impermeant control dye, which increased the risk of misinterpretation. Araya et al. (2005) studied Cx43-based coupling between mononuclear neighbours in primary myoblast cultures and found strong correlations between Cx43 expression, dye transfer and myoblast fusion. Although we confirm their conclusion, that disrupting Cx43 function disrupts both dye transfer and myoblast fusion, our own findings imply that some of the strong dye transfer they observed may have occurred through cytoplasmic, rather than gap-junctional coupling. Similarly, when studying the blocking effects of heptanol on myoblast coupling, using fluorescence recovery after photobleaching (Constantin et al. 1997), the authors were careful to distinguish between the slow exponential recovery caused by dye diffusion from neighbours through gap junctions from the rapid recovery caused by cytoplasmic coupling. However, they did not report on the cytoplasmic coupling, or note any changes in its incidence when heptanol treatment inhibited fusion. The extensive cell coupling through Cx43 channels in the growing fraction of day-2 myoblasts we found, could serve as a pathway for the subsequent growth arrest in myoblasts after which gap junction coupling was downregulated. On this line, inhibited or delayed myoblast fusion when blocking gap junctions (Araya et al. 2005; Constantin et al. 1997; Mege et al. 1994; Proulx et al. 1997),

could also be explained by the inadequate availability of fusion-competent, non-dividing post-mitotic myoblasts at a time, due to unsynchronized cell cycle (Araya et al. 2005).

Manipulation of Cx43 expression in myoblast - the effect of gene transfection on proliferation and fusion

Further exploring the role of Cx43 gap junctions in the regulation of cell-cycle control of maturing myoblasts, we manipulated connexin expression in myoblast cultures in both direction by either increasing or decreasing it to influence GJIC. Cell-cycle-related events were analysed by monitoring cell proliferation and fusion in relation to dye transfer via gap junctions. pIRES2-eGFP constructs for either facilitating or blocking Cx43 expression were transfected into adherent myoblast on day two of culture, prior to the normal peak of cell membrane Cx43 expression. This construct has been introduced earlier with success into retinal precursors by electroporation, in the neural tube in ovo (Becker et al. 2001) and in flat-mounted retinae *in vitro* (Pearson et al. 2004). The sequence encoded by the wtCx43 construct is the original rat Cx43 sequence. The dnCx43 construct encodes a C-terminal-truncated variant that impairs intracellular trafficking to the plasma membrane, and its incorporation into connexon hexamers, imposing a strong functional block even when wild-type protein is present (Becker et al. 2001). In primary myoblast cultures, the transfection reagent Effectene™ gave higher and more consistent yields of GFP^{+} cells than electroporation had done in previous studies, averaging 15% on the day after transfection (day three of culture). However, similar to the earlier studies, the expression of this construct was only transient and on the second day after transfection, GFP could be detected in only about half of the initial fraction (7.5%), and on the third day in only one-eighth (1.7%). However, since the same vector system was used in all of our experiments, and the transfection rates were consistent, the differences between cultures treated with different constructs remain valid as indicators of their functional effects.

Under the conditions of our study, the numbers of GFP^{+} transfected cells in GFP-only and wtCx43 cultures rose by the second day, although less strongly than the total nuclear count, as would be expected in view of the transience of GFP[+] expression. In dnCx43-transfected cultures, however, the number of GFP^{+} cells more than doubled by the second day, and afterwards remained above the peak levels reached by other treatment groups. This striking effect can be attributed to two distinct factors. First, the large increase on the second day can be confidently interpreted as a specific excess of proliferation among dnCx43-transfected cells (and potentially also those untransfected neighbours that could not communicate with

them) because there was also a statistically significant excess in the nuclear count in these cultures, more than the small fraction of cells that were transfected. Secondly, the sustained, large, relative increase in GFP^{+} cells in these cultures on the third and fourth days is a predictable correlate of the highly significant reduction in myotube formation. In support of this interpretation, almost all GFP[+] outlines at these late stages in dnCx43-transfected cultures were mononucleated. Although the effects on proliferation and fusion doubtless interact, they are distinguishable by their separation in time: the reduced fusion in dnCx43-transfected cultures cannot by itself explain the initial large increase in GFP^{+} cells, because fused cells were uncommon, and morphologically identifiable myotubes were absent on the second day after transfection in all treatment groups.

Possible mechanism of action for gap junctions in early myogenesis

According to our findings, a potential role for Cx43 channels in skeletal myogenesis as they promote rapid fusion of myoblasts, would fit into the generally proposed functions of gap junctions e.g. in controlling cell growth for promoting a more differentiated phenotype and/or in coordinating cell functions in a network of cells (Kumar and Gilula, 1996; Trosko and Chang, 2001). How might the functional state of Cx43-based channels regulate syncytium formation? We observed precocious cytoplasmic coupling at pre-fusional stages when wtCx43 is overexpressed, and with the strong fusion-delaying effects of dnCx43. These findings and our correlation of the expression of Cx43 and cell-cycle control proteins suggest that Cx43-based gap junctions may play a role in synchronizing the cycle exit of proliferating myoblast populations to promote their differentiation and rapid fusion. However, synchrony of cycle exit cannot be an absolute prerequisite for fusion because the normal fate of the neonatal satellite cells from which these cultures were derived would have been to fuse asynchronously to adjacent myofibers.

Both unpaired connexons and aligned gap junctions are thought to form important pathways for regulating intracellular Ca^{2+} levels (Goodenough and Paul 2003; Kumar and Gilula 1996), which play a major part in early myogenic differentiation and cell fusion (Constantin et al. 1997; David et al. 1981; Entwistle et al. 1988; Keresztes et al. 1991). Regulation of Ca^{2+} levels via coupling could be involved in the migratory alignment of pre-fusion myoblasts. The coupling of neuronal precursors can coordinate and accelerate their cell-cycle-linked migrations by synchronizing spontaneous transient $[Ca^{2+}]_i$ elevations (Pearson et al. 2004). Although little is known about the control of migration in skeletal myoblasts, that of vascular smooth muscle cells also relies upon spontaneous calcium

transients (Scherberich et al. 2000), which can regulate the calcium/calmodulin-dependent protein kinase II on which their migration depends (Pfleiderer et al. 2004). Calpains (calcium-activated proteases) and their inhibitor, calpastatin, have also been strongly implicated in the control of cytoskeletal reorganization and cell adhesion during myoblast migration and alignment (Dedieu et al. 2004). More generally, $[Ca^{2+}]_i$ levels have a ubiquitous role in regulating actin depolymerization, acting through calcineurin and Slingshot to activate cofilin (Wang et al. 2005). Thus, there are several well-trodden paths by which the gap-junctional coordination of calcium transients could regulate myoblast migration. Besides previously discussed possibilities, coupling via Cx43 gap junction channels may have a direct role in promoting fusion after membrane apposition has occurred, because $[Ca^{2+}]_i$ levels are known to influence the terminal differentiation of myoblasts by several pathways (Araya et al. 2005), all of them potentially sensitive to coupling. In particular, a late $[Ca^{2+}]_i$ elevation step has long been known to be critical for myoblast fusion (Shainberg et al. 1969), and a specific pathway has recently been identified that begins with the activation of Kir2.1 channels and proceeds, by way of hyperpolarization and T-channel opening, to the Ca^{2+}-dependent activation of calcineurin and the expression of the key transcription factors myogenin and MEF2 (Konig et al. 2006). Although fusion-competent myoblasts can activate this pathway cell-autonomously in low-density cultures that lack intercellular coupling (Bernheim et al. 2002), the coupling of a confluent, fusion-competent population could act to synchronize both the hyperpolarization and the Ca^{2+}-dependent effects.

Besides Ca^{2+} level regulation, Cx43 expression and function in differentiating myoblasts could influence signaling pathways, as transient elevation of cAMP, a known positive regulator of Cx43 expression and channel permeability is detected during early myoblast differentiation (Zalin and Montague 1974). Steadily high levels of cAMP, however, interfere with myoblast fusion (Baek et al. 1994), as it was also shown upon treatment of myogenic cells with retinoic acid (Shin et al. 2000), an inducer of cAMP, Cx43 formation and cell coupling (Clairmount and Sies 1997). In addition, the activation of PKC (Farnazeh et al. 1989) and elevated intracellular Ca^{2+} levels (David et al. 1981), both known to be essential for myoblast fusion (David et al. 1990), are demonstrated to close Cx43 channels (Lampe et al. 2000, Kumar and Gilula 1996). In line with this, we showed closure of Cx43 channels in non-manipulated, aligned and prefusion myoblasts just preceeding fusing. However, all of these possibilities may require further investigations.

Conclusion

Taken together, the development of skeletal muscle fibers from mononuclear progenitors is a highly complex series of events requiring the co-operation of large number of cells. For the coordinated cell-membrane fusion of myoblasts, many cells formed in several series of cell cycle need to be tuned to the same differentiation stage. Here we demonstrated *in vivo* and *in vitro*, that the transient upregulation of Cx43 gap junction expression in aligned myoblasts was accompanied by the rapid and synchronized progression of cell cycle control. Our findings suggest that Cx43 gap junctions may mediate this synchronization in prefusion myoblasts to contribute to the coordinated syncytial fusion, during skeletal muscle differentiation.

New observations in our studies:

The main result of our series of experiments, concern the role of GJIC in early myogenesis particularly focusing on myoblast proliferation and fusion. In this respect we gained novel observations by showing:

1. The progressive upregulation of Cx43 gap junction protein in prefusion myoblasts by dissecting pre- and postmitotic stages, and the rapid decline of Cx43 expression after fusion during skeletal muscle differentiation *in vivo* using a rat regeneration model.

2. The spatio-temporal expression of gap junction connexins correlated with the progression of cell cycle control, as the significant upregulation of Cx43 gap junctions in aligned myoblasts preceding fusion was accompanied by the nuclear expression of cyclin-dependent kinase inhibitors $p21^{waf1/Cip1}$ and $p27^{kip1}$ and the complete loss of Ki67 protein.

3. Rat cultured myoblasts showed similar temporal regulation of Cx43 expression and phenotypic maturation to those regenerating *in vivo*. However in prefusion myoblasts we detected extensive GJ coupling between the sparse and proliferating myoblasts and a reduced communication between the aligned, postmitotic cells. This finding functionally supported that that we found in regeneration, namely GJIC has a role in controlling myoblast cell cycle.

4. Myoblasts transfected with wtCx43 showed more gap-junctional coupling than the GFP-only controls, began fusion sooner as judged by the incidence of cytoplasmic coupling, and formed more myotubes. However, myoblasts transfected with dnCx43 remained proliferative for longer than either GFP-only or wtCx43 myoblasts, showed less coupling, and underwent little fusion into myotubes. These results further confirmed the role of gap junction direct cell-cell communication in controlling and probably synchronising myoblast cell cycle for a coordinated syncytial fusion.

References

1. Alves LA, Coutinho-Silva R, Persechini PM, Spray DC, Savino W, Campos de Carvalho AC (1996) Are there functional gap junctions or junctional hemichannels in macrophages? Blood 88:328-334

2. Araya R, Eckhardt D, Maxiener S, Kruger O, Theiss M, Willecke K, Saez JC (2005) Expression of connexins during differentiation and regeneration of skeletal muscle: functional relevance of connexin43. J Cell Sci 118: 27-37

3. Azzam EI, de Toledo SM, Little JB (2001) Direct evidence for the participation of gap junction-mediated intercellular communication in the transmission of damage signals from alpha -particle irradiated to non-irradiated cells. Proc Natl Acad Sci 98:473-478

4. Baek HJ, Jeon YJ, Kim HS, Kang MS, Chung CH, Ha DB (1994) Cyclic AMP negatively modulates both Ca^{2+}/calmodulin-dependent phosphorylation of the 100-kDa protein and membrane fusion of chick embryonic myoblasts. Dev Biol 165:178-184

5. Balogh S, Naus CC, Merrifield PA (1993) Expression of gap junctions in cultured rat L6 cells during myogenesis Dev Biol 155:351-360

6. Beardslee MA, Laing JG, Beyer EC, Saffitz JE (1998) Rapid turnover of connexin43 in the adult rat heart. Circ Res 83:629-635

7. Beauchamp JR, Heslop L, Yu DS, Tajbakhsh S, Kelly RG, Wernig A, Buckingham ME, Partridge TA, and Zammit PS (2000) Expression of CD34 and myf5 defines the majority of quiescent adult skeletal muscle satellite cells. J Cell Biol 151:1221–1234

8. Becker DL, Ciantar D, Catsicas M, Pearson R, Mobbs P (2001) Use of pIRES vectors to express eGFP and connexin constructs in studies of the role of gap junctional communication in the early development of the chick retina and brain. Cell Commun Adhes 8:355–359

9. Becker DL, Evans WH, Green CR, Warner A (1995) Functional analysis of amino acid sequences in connexin43 involved in intercellular communication through gap junctions. J Cell Sci 108:1455-1467

10. Becker DL, McGonnell I, Makarenkova HP, Patel K, Tickle C, Lorimer J, Green CR. (1999) Roles for alpha 1 connexin in morphogenesis of chick embryos revealed using a novel antisense approach. Dev Genet. 24:33-42

11. Bergoffen J, Scherer SS, Wang S, Oronzi SM, Bone LJ, Paul DL, Chen K, Lensch MW, Chance PF, Fishbeck KH (1993) Connexin mutations in X-linked Charcot-Marie-Tooth disease. Science 262:2039-2042

12. Bernheim L, Bader CR (2002) Human myoblast differentiation: Ca^{2+} channels are activated by K^+ channels. News Physiol Sci 17:22–26

13. Berthoud VM, Singh R, Minogue PJ, Ragsdale CW, Beyer EC (2004) Highly restricted pattern of connexin36 expression in chick somite development. Anat Embryol (Berl) 209:11-18

14. Beyer EC (1990) Molecular cloning and developmental expression of two chick embryo gap junction proteins. J Biol Chem 265:14439-14443

15. Bischoff R (1990) Cell cycle commitment of rat muscle satellite cells. J Cell Biol 111:201-207

16. Brustis JJ, Elamrani N, Balcerzak D, Safwate A, Soriano M, Poussard S, Cottin P, Ducastaing A (1994) Rat myoblast fusion requires exteriorized m-calpain activity. Eur J Cell Biol 64(2):320-7

17. Bruzzone R, White TW, Paul DL (1996) Connections with connexins: the molecular basis of direct intercellular signalling. Eur J Biochem 238:1–27

18. Bukauskas FF, Kempf C, Weingart R(1992) Cytoplasmic bridges and gap junctions in an insect cell line (Aedes albopictus). Exp Physiol 77:903–911

19. Cantini M, Giurisato E, Radu C, Tiozzo S, Pampinella F, Senigaglia D, Zaniolo G, Mazzoleni F, Vitiello L (2002) Macrophage-secreted myogenic factors: a promising tool for greatly enhancing the proliferative capacity of myoblasts in vitro and in vivo. Neurol Sci 23:189-194

20. Chandross KJ, Kessler JA, Cohen RI, Simburger E, Spray DC, Bieri P, Dermietzel R (1996) Altered connexin expression after peripheral nerve injury. Mol Cell Neurosci 7:501-518

21. Charge SBP, Rudnicki MA (2004) Cellular and molecular regulation of muscle regeneration. Physiol Rew 84:209-238

22. Cheng A, Tang H, Cai J, Zhu M, Zhang X, Rao M, Mattson MP (2004) Gap junctional communication is required to maintain mouse cortical neural progenitor cells in a proliferative state. Dev Biol 272:203–216

23. Choi SW, Baek MY, Kang MS (1992) Involvement of cyclic GMP int he fusion of chick embryonic myoblasts in culture. Exp Cell Res 199:129-133

24. Christ B, Ordahl CP (1995) Early stages of chick somite development. Anat Embryol 191:381–396

25. Clairmount A, Sies H (1997) Evidence for posttranscriptional effect of retinoic acid on connexin43 gene expression via the 3'-untranslated region. FEBS Lett 419:268-270

26. Constantin B, Cronier L (2000) Involvement of gap junctional communication in myogenesis. Int Rev Cytol 196:1-65

27. Constantin B, Cronier L, Raymond G (1997) Transient involvement of gap junctional communication before fusion of newborn rat myoblasts. C R Acad Sci III 320:35-40

28. Cossu G and Molinaro M (1987) Cell heterogeneity in the myogenic lineage. Curr Top Dev Biol 23: 185–208

29. Crow DS, Beyer EC, Paul DL, Kobe SS, Lau AF (1990) Phosphorylation of Connexin43 Gap Junction Protein in Uninfected and Rous-Sarcoma Virus-Transformed Mammalian Fibroblasts. Mol Cell Biol 10:1754-1763

30. Dahl E, Winterhager E, Traub O, Willecke K (1995) Expression of gap junction genes, connexin40 and connexin43, during fetal mouse development. Anat Embryol (Berl) 191:267-278

31. David JD, Higginbotham CA (1981) Fusion of chick embryo skeletal myoblasts: interactions of prostaglandin E1, adenosine 3':5' monophosphate, and calcium influx. Dev Biol 82(2):308-16

32. David JD, See WM, Higginbotham CA (1981) Fusion of chick embryo skeletal myoblasts: role of calcium influx preceding membrane union. Dev Biol 82(2):297-307

33. David JD, Faser CR, Perrot GP (1990) Role of protein kinase C in chick embryo skeletal myoblast fusion. Dev Biol 139:89-99

34. De Maio A, Vega VL, Contreras JE (2002) Gap Junctions, Homeostasis, and Injury. J Cell Physiol 191:269–282

35. Dermietzel R, Hwang TK, Spray DS (1990) The gap junction family: structure, function and chemistry. Anat Embryol 182:517–528

36. Dietrich S, Abou-Rebyeh F, Brohmann H, Bladt F, Sonnenberg-Riethmacher E, Yamaai T, et al. (1999) The role of SF/HGF and c-Met in the development of skeletal muscle. Development 126:1621–1629

37. Dedieu S, Poussard S, Mazères G, Grise F, Dargelos E, Cottin P, Brustis JJ (2004) Myoblast migration is regulated by calpain through its involvement in cell attachment and cytoskeletal organization. Exp Cell Res 292:187–200

38. Doble BW, Kardami E (1995) Basic fibroblast growth factor stimulates connexin-43 expression and intercellular communication of cardiac fibroblasts Mol Cell Biochem 143(1):81-7

39. Duffy HS, Delmar M, Spray DC (2002) Formation of the gap junction nexus: binding partners for connexins. J Physiol 96:243–249

40. Duxson MJ, Usson Y (1989) Cellular insertion of primary and secondary myotubes in embryonic rat muscles. Development 107:243–251

41. Edom-Vovard F, Bonnin MA, Duprez D (2001) Misexpression of Fgf4 in the chick limb inhibits myogenesis by down-regulating Frek expression. Dev. Biol. 233:56–71

42. Entwistle A, Zalin RJ, Bevan S, Warner AE (1988) The control of chick myoblast fusion by ion channels operated by prostaglandins and acetylcholine. J Cell Biol 106:1693-1702

43. Eugenin EA, Branes MC, Berman JW, Saez JC (2003) TNF-alpha plus IFN-gamma induce connexin43 expression and formation of gap junctions between human monocytes/ macrophages that enhance physiological responses. J Immunol 170:1320-1328

44. Evans WH (1994) Assembly of Gap Junction Intercellular Communication Channels. Biochem Soc Transact 22:788-792

45. Evans WH, Martin PE (2002) Gap junctions: structure and function (Review). Mol Membr Biol 19(2):121-36

46. Fallon RF, Goodenough DA (1981) Five-hour half-life of mouse liver gap-junction protein. J Cell Biol 90(2):521

47. Farnazeh F, Entwistle A, Zalin RJ (1989) Protein kinase C mediates the hormonally regulated plasma membrane fusion of avian embryonic skeletal muscle. Exp Cell Res 181:298-304

48. Friday BB, Horsley V, Pavlath GK (2000) Calcineurin activity is required for the initiation of skeletal muscle differentiation. J Cell Biol 149:657-666

49. Goodenough DA, Goliger JA, Paul DL (1996) Connexins, connexons, and intercellular communication. Ann Rev Biochem 65:475-502

50. Goodenough DA, Paul DL (2003) Beyond the gap: functions of unpaired connexon channels. Nat Rev Mol Cell Biol 4:285-294

51. Goodenough DA, Paul DL, Beyer EC (1988) The Connexins - a Family of Gap Junction Proteins. Biophys J 53:A34

52. Haider SR, Wang W, Kaufmann SJ (1994) SV40T antigen inhibits expression of MyoD and myogenin, up-regulates myf-5, but does not affect early expression of desmin or α7 integrin during muscle development. Exp Cell Res 210:278-286

53. Harris JB, Johnson MA, Karlsson E (1975) Pathological responses of rat skeletal muscle to a single subcutaneous injection of a toxin isolated from the venom of the Australian tiger snake Notechis scutatus scutatus. Clin Exp Pharm Physiol 2:383-404

54. Hawke TJ, Garry DJ (2001) Myogenic satellite cells: physiology to molecular biology. J Appl Physiol 91:534-551

55. Kalderon N, Epstein ML, Gilula NB (1977) Cell-to-cell communication and myogenesis. J Cell Biol 75:788-806

56. Kamei J, Toyofuku T, Hori M (2003) Negative regulation of p21 by beta-catenin/TCF signaling: a novel mechanism by which cell adhesion molecules regulate cell proliferation. Biochem Biophys Res Comm 312:380–387

57. Kaufmann U, Martin B, Link D, Witt K, Zeitler R, Reinhard S, Starzinski-Powitz A (1999) M-cadherin and its sisters in development of striated muscle. Cell Tissue Res 296:191-198

58. Keresztes M, Haggblad J, Heilbronn E (1991) Basal and ATP-stimulated phosphoinositol metabolism in fusing rat skeletal muscle cells in culture. Exp Cell Res 196:362-364

59. Kidder GM, Winterhager A (2001) Intercellular communication in preimplantation development: the role of gap junctions. Front Biosci 6:D731-6

60. Kimura H, Oyadama Y, Ohshika H, Mori M, Oyamada M (1995) Reversible inhibition of gap junctional intercellular communication, synchronous contraction, and synchronism of intracellular Ca2+ fluctuation in cultured neonatal rat cardiac myocytes by heptanol. Exp Cell Res 220(2):348-56

61. Kitzmann M, Fernandez A (2001) Crosstalk between cell cycle regulators and the myogenic factor MyoD in skeletal myoblasts. Cell Mol Life Sci 58:571-579

62. Ko K, Arora P, Lee W, McCulloch C (2000) Biochemical and functional characterization of intercellular adhesion and gap junctions in fibroblasts. Am J Physiol Cell Physiol 279:C147-157

63. Koffer L, Roshong S, Park IK, Cesen-Cummings K, Thopson DC, Dwyer-Nield, Rice P, Mamay C, Malkinson AM, Ruch RJ (2000) Growth inhibition in G1 and altered expression of cyclin D1 and p27[kip1] after forced connexin expression in lung and liver carcinoma cells. J Cell Biochem 79:347-354

64. Konig S, Béguet A, Bader CR, Bernheim L (2006) The calcineurin pathway links hyperpolarization (Kir2.1)-induced Ca^{2+} signals to human myoblast differentiation and fusion. Development 133:3107–3144

65. Krenacs L, Krenacs T, Raffeld M (1999) Antigen retrieval for immunohistochemical reactions in routinely processed paraffin sections. Methods Mol Biol 115:85-93

66. Kumar NM, Gilula NB (1996) The gap junction communication channel. Cell 84:381-388

67. Laird DW (1996) The life cycle of a connexin: Gap junction formation, removal, and degradation. J Bioenerg Biomembr 28:311-318

68. Laird DW, Castillo M, Kasprzak L (1995) Gap Junction Turnover, Intracellular Trafficking, and Phosphorylation of Connexin43 in Brefeldin-a-Treated Rat Mammary-Tumor Cells. J Cell Biol 131:1193-1203

69. Lampe PD, TenBroek EM, Burt JM, Kurata WE, Johnson RG (2000) Phosphorylation of connexin43 on serine368 by protein kinase C regulates gap junctional communication. J Cell Biol 149:1503-1512

70. Lawlor MA, Rotwein P (2000) Coordinate control of muscle cell survival by distinct insulin-like growth factor activated signaling pathways. J Cell Biol 151:1131-1140

71. Lefaucheur JP, Sebille A (1995) The cellular events of injured muscle regeneration depend on the nature of the injury. Neuromuscul Disord 5:501-509

72. Lescaudron L, Peltekian E, Fontaine-Perus J, Paulin D, Zampieri M, Garcia L, Parrish E (1999) Blood borne macrophages are essential for the triggering of muscle regeneration following muscle transplant. Neuromuscul Disord 9:72-80

73. Liao Y, Day KH, Damon DN, Duling BR (2001) Endothelial cell-specific knockout of connexin 43 causes hypotension and bradycardia in mice. Proc Natl Acad Sci 98:9989-9994

74. Little JB, Azzam EI, de Toledo SM, Nagasawa H (2002) Bystander effects: intercellular transmission of radiation damage signals. Radiat Prot Dosimetry 99:159-162

75. Loewenstein WR (1981) Junctional intercellular communication: the cell-to-cell membrane channel. Physiol Rev 1981 61(4):829-913

76. Loewenstein WR, Rose B (1992) The cell-cell channel in the control of growth. Semin Cell Biol 3:59–79

77. Mege RM, Goudou D, Giaume C, Nicolet M, Rieger F (1994) Is intercellular communication via gap junctions required for myoblast fusion? Cell Adhes Commun 2:329-343

78. Mendler L, Zador E, Dux L, Wuytack F (1998) mRNA levels of myogenic regulatory factors in rat slow and fast muscles regenerating from notexin-induced necrosis. Neuromuscul Disord 8:533–541

79. Mignon C, Fromaget C, Mattei MG, Gros D, Yamasaki H, Mesnil M (1996) Assignment of connexin 26 (GJB2) and 46 (GJA3) genes to human chromosome 13q11->q12 and mouse chromosome 14D1-E1 by in situ hybridization. Cytogen Cell Genet 72:185-186

80. Milks LC, Kumar NM, Houghten R, Unwin N, Gilula NB (1988) Topology of the 32-Kd Liver Gap Junction Protein Determined By Site- Directed Antibody Localizations. Embo J 7:2967-2975

81. Ostrovsky O, Bengal E (2003) The mitogen-activated protein kinase cascade promotes myoblast cell survival by stabilizing the cyclin-dependent kinase inhibitor, p21WAF1 protein. J Biol Chem 278:21221-21231

82. Parker MH, Seale P, Rudnicki MA (2003) Looking back to the embryo: defining transcriptional networks in adult myogenesis. Nat Rev Genet 4:497-507

83. Paul DL (1995) New functions for gap junctions. Curr Opin Cell Biol 5:665-72

84. Pearson R, Catsicas M, Becker DL, Bayley P, Lunebörg N, Mobbs P (2004) Ca^{2+} signalling and gap junction coupling within and between pigment epithelium and neural retina in the developing chick. Eur J Neurosci 19:2435–2445

85. Pfleiderer PJ, Lu KK, Crow MT, Keller RS, Singer HA (2004) Modulation of vascular smooth muscle cell migration by calcium/calmodulin-dependent protein kinase II-delta2. Am J Physiol Cell Physiol 286:C1238–C1245

86. Proulx A, Merrifield PA, Naus CC (1997) Blocking gap junctional intercellular communication in myoblasts inhibits myogenin and MRF4 expression. Dev Genet 20:133-144

87. Rando TA, Blau HM (1994) Primary mouse myoblast purification, characterization and transplantation for cell-mediated gene therapy. J Cell Biol 125:1275-1287

88. Rash JE, Fambrough D (1973) Ultrastructural and eletrophysiological correlates of cell coupling and cytoplasmic fusion during myogenesis in vitro. Dev Biol 30:166-186

89. Rash JE, Staehelin LA (1974) Freeze-cleave demonstration of gap junctions between skeletal myogenic cells in vivo. Dev Biol 36:455-61

90. Rawls A, Olson EN (1997) MyoD meets its maker. Cell 89:5-8

91. Robertson TA, Maley MA, Grounds MD, Papadimitriou JM (1993) The role of macrophages in skeletal muscle regeneration with particular reference to chemotaxis. Exp Cell Res 207:321-331

92. Rudnicki MA, Schnegelsberg PN, Stead RH, Braun T, Arnold HH, Jaenisch R (1993) MyoD or Myf-5 is required for the formation of skeletal muscle. Cell 75:1351-1359

93. Scherberich A, Campos-Toimil M, Rondé P, Takeda K, Beretz A (2000) Migration of human vascular smooth muscle cells involves serum-dependent repeated cytosolic calcium transients. J Cell Sci 113:653–662

94. Schmalbruch H (1982) Skeletal muscle fibers of newborn rats are coupled by gap junctions. Dev Biol 91:485-490

95. Seale P, Sabourin LA, Girgis-Gabardo A, Mansouri A, Gruss P, and Rudnicki MA (2000) Pax7 is required for the specification of myogenic satellite cells. Cell 102:777–786

96. Severs NJ (1999) Cardiovascular disease. Novartis Found Symp 219:188-206

97. Shainberg G, Yagil D, Yaffe (1969) Control of Myogenesis in vitro by Ca concentration in nutritional medium. Exp Cell Res 58:163-167

98. Sherr CJ, Roberts JM (1999) CDK inhibitors: positive and negative regulators of G_1-phase progression. Gen Devel 13:1501-1512

99. Shin YJ, Woo JH, Chung CH, Kim HS (2000) Retinoic acid and its geometrical isomers block both growth and fusion of L6 myoblasts by modulating the expression of protein kinase A. Mol Cells 10:162-168

100. Simon AM, Goodenogh DA (1998) Diverse functions of vertebrate gap junctions. Trends Cell Biol 8(12):477-Becker DL, Leclerc-David C, Warner A (1992) The relationship of gap junctions and compaction in the preimplantation mouse embryo. Dev Suppl 113-8

101. Söhl G, Willecke K (2003) An update on connexin genes and their nomenclature in mouse and man. Cell Commun Adhes 10:173–180

102.   Sosinsky GE (1996) Molecular organization of gap junction membrane channels J Bioenerg Biomemr 28:297-309

103.   Stock A, Sies H (2000) Thyroid hormone receptors bind to an element in the connexin43 promoter. Biol Chem 381(9-10):973-9

104.   Tajbakhsh S (2003) Stem cells to tissue: molecular, cellular and anatomical heterogeneity in skeletal muscle. Curr Op inGen and Dev 13:413-422

105.   Tajbakhsh S, Buckingham M (2000) The birth of muscle progenitor cells in the mouse: spatiotemporal considerations. Current Topics in Developmental Biology, Somitogenesis 47:225–268

106.   Tajbakhsh S, Buckingham ME (1994) Mouse limb muscle is determined in the absence of the earliest myogenic factor myf-5. Proc Natl Acad Sci USA 91:747–751

107.   Tajbakhsh S, Rocancourt D, Buckingham M (1996) Muscle progenitor cells failing to respond to positional cues adopt non-myogenic fates in myf-5 null mice. Nature 384:266–270

108.   Trosko JE, Chang CC (2001) Mechanism of up-regulated gap junctional intercellular communication during chemoprevention and chemotherapy of cancer. Mutat Res 480-481:219-229

109.   Von Maltzahn J, Euwens C, Willecke K, Sohl G (2004) The novel mouse connexin 39 gene is expressed in developing striated muscle fibers J Cell Sci 117:5381-5392

110.   Walsh K, Perlman H (1997) Cell cycle exit upon myogenic differentiation. Curr Opin Genet Dev. 7:597-602

111.   Wang Y, Shibasaki F, Mizuno K (2005) Calcium signal-induced cofilin dephosphorylation is mediated by Slingshot via calcineurin. J Biol Chem 280:12683–12689

112.   Webb SE, Lee KKH, Tang MK, Ede DA (1997) Fibroblast growth factors 2 and 4 stimulate migration of mouse embryonic limb myogenic cells. Dev Dynamics 209:206–216

113.   Willecke K, Eiberger J, Degen J, Eckardt D, Romualdi A, Guldenagel M, Deutsch U, Sohl G (2002) Structural and functional diversity of connexin genes in the mouse and human genome. Biol Chem 383:725-737

114.   Willecke K, Hennemann H, Jungbluth S, Heynkes R (1991) The diversity of connexin genes encoding gap junctional proteins. Eur J Cell Biol 56(1):1-7

115.   Yun K, Wold B (1996) Skeletal muscle determination and differentiation: story of a core regulatory network and its content. Curr Opin Cell Biol 8:877-889

116.   Zador E, Mendler L, Ver Heyen M, Dux L, Wuytack F (1996) Changes in mRNA levels of the sarcoplasmic/endoplasmic-reticulum Ca(2+)-ATPase isoforms in the rat soleus muscle regenerating from notexin-induced necrosis. Biochem J 320:107-113

117.   Zalin RJ, Montague W (1974) Changes in adenylate cyclase, cyclic AMP, and protein kinase levels in chick myoblasts, and their relationship to differentiation. Cell 2:103-108